IEEE Access
Multidisciplinary ⋮ Rapid Review ⋮ Open Access Journal

Received 16 March 2023, accepted 7 April 2023, date of publication 14 April 2023, date of current version 31 August 2023.

Digital Object Identifier 10.1109/ACCESS.2023.3267110

RESEARCH ARTICLE

A Novel Meta-Heuristic Algorithm for Numerical and Engineering Optimization Problems: Piranha Foraging Optimization Algorithm (PFOA)

SHUAI CAO[1,2,3], **QIAN QIAN**[1,2], **YONGJUN CAO**[1,3,4], **WENWEI LI**[4], **WEIXI HUANG**[4], **AND JIANAN LIANG**[4]

[1]Faculty of Information Engineering and Automation, Kunming University of Science and Technology, Kunming 650500, China
[2]Key Laboratory of Computer Technology Application of Yunnan Province, Kunming 650500, China
[3]Guangdong Key Laboratory of Modern Control Technology, Institute of Intelligent Manufacturing, Guangdong Academy of Sciences, Guangzhou 510070, China
[4]Robotic Laboratory, South China Robotics Innovation Research Institute, Foshan 528300, China

Corresponding author: Qian Qian (2910099768@qq.com)

This research was partially supported by the Research and application of intelligent scheduling for mobile cooperative robot cluster oriented to Intelligent manufacturing (2130218003022) Foshan Science and Technology Innovation Team Project under Grant FS0AA-KJ919-4402-0060, in part by the Study on Cognitive Mechanism of temporal effect of visual Attention shift of NSFC. 32060193.

ABSTRACT This paper provides a novel meta-heuristic optimization algorithm for solving continuous optimization problems efficiently in the field of numerical and engineering optimization: Piranha Foraging Optimization Algorithm (PFOA). The algorithm is inspired by the flexible and mobile foraging behavior of piranha swarm and divides their foraging behavior into three patterns: localized group attack, bloodthirsty cluster attack and scavenging foraging, simulates the above behaviors to construct two dynamic search processes for exploration and exploitation. PFOA uses three strategies of non-linear parameter control, population survival and reverse evasion search to enable populations to have better population diversity at different stages of the search and to help find better solutions. To gain insight into the performance of PFOA, visualization methods were used to assess the efficiency of PFOA optimization and to analyse the impact of the characteristics of the three foraging modes, the sensitivity of the parameters and the size of the piranha population on the algorithm. The algorithm performance was further tested with 27 CEC benchmark functions and four real engineering design optimization problems, and the results were compared with 13 well-known meta-heuristics. Test results based on statistical methods such as box-line plots, Wilcoxon rank sum test and Friedman test in multiple dimensions (30, 50, 100 and fixed dimensions) show significant differences compared to other algorithms and that the performance of the algorithm is stable and in significant improvement. The unique advantages of PFOA in terms of the equilibrium of convergence speed and exploration can avoid getting trapped in local optimum regions and effectively solve optimization problems in complex search spaces.

INDEX TERMS Meta-heuristic algorithms, piranha foraging optimization algorithm (PFOA), swarm intelligence, bionic inspired algorithms.

I. INTRODUCTION

Optimization is the process of finding an optimal solution to a given system from all possible values, such that the output is maximized or minimized. Optimization problems such as engineering design [1], AGV path planning and scheduling [2], wireless sensors [3], and computer image processing [4] are difficult for traditional methods to find optimal solutions in complex search spaces containing multiple local traps due to multiple independent variables, complex constraints, and mathematical properties that are non-linear in nature. Coupled with the rapid development of artificial intelligence and big data, the scale of engineering optimization problems is increasing and a "combinatorial explosion"

The associate editor coordinating the review of this manuscript and approving it for publication was Diego Oliva.

is occurring. In this context, Meta-heuristic Algorithms (MA) have attracted a lot of attention and In-depth research due to their high execution efficiency, low parameters, high search capability and lack of dependence on the gradient information (integration or derivative) of the objective function in solving complex optimization problems [5].

After decades of development, Meta-heuristic algorithms have evolved into different branches. The first category is Swarm Intelligence Algorithms (SI), which Bonabeau [6] defines as ''the collective intelligence that arises from a group of simple biological individuals''. SI is based on optimization algorithms that simulate foraging, cooperative transport, nesting and other social behaviors of insects, plants or mammals. The self-organizing nature of the swarm and the natural division of labour are two essential attributes of SI. Swarm self-organization is the ability of a system to organize itself from individuals to groups without any external help; natural division of labour is the ability of a population to coordinate the division of labour among individuals and to cooperate in solving complex problems. Two key features of group intelligence make groups highly self-organizing and adaptive, and exhibit non-linear system characteristics. Among the typical SI algorithms are, Particle Swarm Optimization Algorithm (PSO) [7], Honey Badger Algorithm (HBA) [8], and Chameleon Swarm Algorithm (CSA) [9]. The second category is Evolutionary Algorithms (EA). In nature, organisms evolve and develop from lower to higher levels through a series of heredity, selection and mutation, and people have modeled the essence of this ''survival of the fittest'' evolutionary law to form an optimization algorithm, the evolutionary algorithm. Evolutionary Algorithms are a range of search techniques which include Genetic Algorithms (GA) [10], Differential Evolutionary Algorithms (DE) [11], evolutionary planning [12], evolutionary strategies [13], etc. The third category is The simulation of natural scientific principles and phenomena algorithms(NP), as the name suggests, is based on the simulation of scientific principles and phenomena, of which the representative ones are Simulated Annealing Algorithm (SA) [14] and Thermal Exchange Optimization Algorithms (TEO) [15].

Meta-heuristic algorithms have been used in a wide variety of fields due to their unique computational mechanism, but they also suffer from certain drawbacks. Firstly, meta-heuristic algorithms are based on heuristic rules and randomness to find the optimal solution, but sometimes these rules and randomness can lead the algorithm into a local optimility trap and thus fail to find the global optimal solution. Secondly, meta-heuristics algorithms usually require a large number of iterations, resulting in long running times and slow convergence. Thirdly, meta-heuristic algorithms usually have multiple parameters, and the tuning of these parameters has a large impact on the performance of the algorithm, and tuning these parameters usually requires a lot of experimentation and experience and is more difficult to adjust. To optimize the above, there are now three research paths. First, to propose new meta-heuristic algorithms with stronger search performance, for example, Dingo Optimization Algorithm (DOA) [16], Honey Badger Algorithm (HBA) [17], Smell Agent Optimization (SAO) [18], Chimp Optimization Algorithm (CHOA) [19], Rat Swarm Optimization (RSO) [20]. Second, to fuse existing optimization algorithms to enhance the global search capability of the algorithms, for example, Harris Hawks Optimization and Differential Evolution (HHOA-DE) [21], Immune Genetic Algorithm and Particle Swarm Optimization (IGV-PSO) [22], Beetle antenna strategy based grey wolf optimization (BGWO) [23]. Third, to improve the existing meta-heuristic algorithms by introducing multiple search strategies and operational mechanisms to enhance the algorithm's search capability. of which, 1. Introducing a chaotic mapping mechanism in the initialization process to generate a highly random and disordered sequence of values as the initial population, thus improving the global search capability and optimization accuracy of the algorithm, such as Bird Swarm Algorithms with Chaotic Mapping [24] 2. Improving the convergence speed and convergence performance of the algorithm by introducing a specific diversity strategy and a specific convergence strategy. [25] 3. Using an adaptive weighting mechanism to generate different search agents according to their [26] 4. Multi-objective strategies are introduced to improve the population diversity and global search capabilities of the algorithm [27].

On the one hand, according to the above literature, population-based meta-heuristic algorithms still suffer from slow convergence, weak global exploitation, and tend to fall into local optimum regions waiting for optimization questions, which points to research directions for exploring new swarm intelligence algorithms in the future. On the other hand, in terms of the logic of the No Free Lunch Theorem (NFL) [28], the mathematical model complexity changes in response to changes in the engineering optimization problem, and it is difficult for a single algorithm to accommodate both global and local searches, so no meta-heuristic algorithm can solve all optimization problems. These two reasons are what prompted us to propose a new meta-heuristic algorithm for modelling piranha foraging behavior:The Piranha Foraging Optimization Algorithm (PFOA).

This paper investigates the outstanding problems of existing swarm intelligence optimization algorithms such as slow convergence, the tendency to fall into local optimum regions, resulting in premature maturity of the algorithm and the loss of search power due to the non-smooth transition between global and local search, etc. The main contributions are as follows:

1) A meta-heuristic algorithm for modelling piranha foraging behavior is proposed: The Piranha Foraging Optimization Algorithm (PFOA).
2) The use of the blood concentration parameter (F) to direct piranhas to identified potential search areas effectively ensures the exploitability of the stock.

3) Dynamic time-varying randomization using a non-linear cosine factor (S) to smoothly transition exploration behavior to exploitation behavior.
4) The reverse escape search strategy uses flags (E) to change the search direction of the population, avoiding the population candidates being trapped in local search regions and further optimizing and improving the solution by directing the search agents to new regions. This approach will continue throughout the algorithm, so that even when the end of the iteration is reached, there is still the possibility of finding a better position.

The paper is structured as follows: The first part presents the background to the development of meta-heuristics, the existing problems and the current state of research; The second section is an introduction to the new algorithm, including mathematical modelling and parametric analysis; The third section is the classification experiments of our algorithm, which verified the effectiveness of it by comparing and analyzing the results with more than 10 excellent swarm intelligence algorithms; In the fourth section, the algorithm is applied to four engineering design examples to verify its general applicability; The fifth and sixth section is the conclusion, which summarizes the work of this paper and the prospects of the algorithm.

II. PIRANHA FORAGING OPTIMIZATION ALGORITHM (PFOA)

This section discusses the inspiration and mathematical model for the piranha foraging optimization algorithm.

A. PIRANHAS IN BIOLOGY

Piranhas [29], [30] are cold-blooded killers widely distributed in the Amazon rivers of South America and are widely known for their highly aggressive qualities. There are currently around 56 species of piranhas worldwide, all of which belong to the family Liparidae, the most aggressive of which are found in the Amazonian rivers of Latin America. They are usually no more than 30cm long, but have a distinctive appearance, with a flattened neck and slightly bulging back, bloodthirsty scarlet eyes, a thick skull and a surprisingly strong bite, and serrated teeth that can easily bite through the animal's flesh [31]. The dorsum is heavily coloured, appearing dark green and gradually lightening in colour from top to bottom, with the lowermost part of the belly appearing bright red, as shown in Figure.1(a). Female piranhas spawn during the rainy season, laying up to a thousand sticky eggs at a time, which use the roots or leaves of plants in the water as incubation beds. However, whenever Amazonian rivers flood, large numbers of piranha eggs are washed elsewhere or sink to the bottom, which makes piranha hatching rates not very high [32].

(a) (b)

FIGURE 1. Piranhas in biology.

Piranhas are very aggressive and often use swarming attacks when attacking their prey, (Figure.1(b)). Once targeted, all members take turns to attack and bite their prey, their powerful jaws and sharp teeth, combined with their powerful fins, can rip off around 15cm of flesh in no time, and the blood of their prey attracts nearby shoals of piranhas to enjoy the feast. It is widely accepted by the scientific community that piranhas rely primarily on hearing and extreme sensitivity to the smell of blood to hunt their prey. Its vision is very poor and at night or in the more turbid Amazonian rivers they can barely see prey beyond 25cm. In this case, having to swim alone in their habitat and rely on foraging for some carrion and seeds to survive, the single piranhas become very timid and have none of their usual swarming, strutting presence.

B. MATHEMATICAL MODEL OF PFOA

The PFOA algorithm defines three patterns of localized group attack, bloodthirsty cluster attack and scavenging foraging, and its steps consist mainly of population initialization, population evaluation and parameter and agent position updating.

In the PFOA algorithm, the set of population candidate solutions can be expressed as:

$$x = \begin{bmatrix} x_{11} & x_{12} & x_{13} & \dots & x_{1D} \\ x_{21} & x_{22} & x_{23} & \dots & x_{2D} \\ & \dots & \dots & \dots & \\ x_{(n-1)1} & x_{(n-1)2} & x_{(n-1)3} & \dots & x_{(n-1)D} \\ x_{n1} & x_{n2} & x_{n3} & \dots & x_{nD} \end{bmatrix}$$

$x_i = \left[x_{i1} \; x_{i2} \; \dots \; x_{iD} \right]$ Position vector representing piranhas.

STEP 1 Population initialization: Initialize the position vector of each individual in the piranha population according to Eq. (1).

$$x_i = lb_i + \beta_1 \times (ub_i - lb_i) \tag{1}$$

where x_i is the location of the i th individual in the piranha candidate solution, ub_i and lb_i represent the upper and lower boundaries of the piranha search in the habitat, respectively. β_1 denotes a random number between 0 and 1.

STEP 2 Define the predation intensity parameter F: Piranhas are extremely sensitive to the detection of blood, a characteristic that is influenced by both the blood concentration F_i and the distance d_i between the prey and the piranha. The spread of blood concentration satisfies the inverse square law model in Figure 2. Piranhas will swim towards areas of high blood concentration, and the higher the blood concentration, the faster their movement, and vice versa, yielding the following Eq. (2).

$$\begin{aligned} F_i &= \beta_2 \times \frac{Z_i}{4\pi d_i^2} \\ d_i &= x_{prey} - x_i \\ Z_i &= [x_i(t) - x_{i+1}(t)]^2 \end{aligned} \tag{2}$$

where F_i denotes the predation intensity parameter for the location of the i th individual piranha, d_i denotes the distance between the position of the i-th individual piranha and the prey (optimal solution), Z denotes the source intensity (e.g. the location of the prey in Figure 2), Z_i denotes the source intensity perceived by the i-th search agent, which will change in real time as the agents continue to follow, and β_2 denotes a random number between 0 and 1.

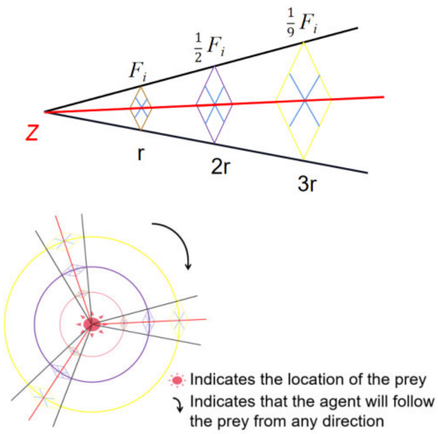
F_i
$\frac{1}{2}F_i$
$\frac{1}{9}F_i$
Z
r
2r
3r
Indicates the location of the prey
Indicates that the agent will follow the prey from any direction

FIGURE 2. Application of inverse square law in Eq. (2).

STEP 3 Non-linear parametric control strategies: Non-linear parametric control strategies are effective measures used to control time-varying randomized processes and prevent premature convergence of populations while ensuring a smooth and silky transition between exploration and exploitation. In the early and middle stages of PFOA, larger values of S help the search agent to perform an auditory-based global search and avoid getting stuck in a local optimum, while in the later stages, PFOA can converge faster as S changes, see Eq. (3).

$$S = C \cdot \cos\left[\frac{\pi}{2} \otimes \left(\frac{t}{Max\_iter}\right)\right]^4 \tag{3}$$

where Max_iter denotes the maximum number of iterations and the constant C is verified (taken as 5 by default), $\otimes$ denotes the product of a value and a variable.

STEP 4 Reverse escape search strategy: In this paper, the reverse escape search strategy is to use flag E to change the direction of the population search, not allowing the candidate population to be trapped in a local area and directing the search to a new area to further improve the solution. This happens frequently throughout the search process, which gives the search agent more opportunities to carefully and rigorously scan the search area, see Eq. (4)

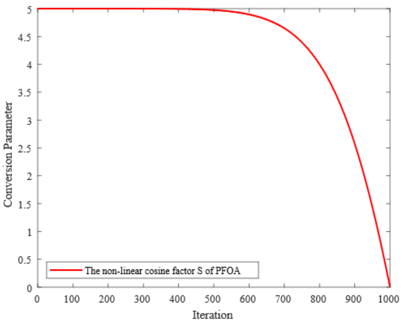

FIGURE 3. Curves for the non-linear control parameter S.

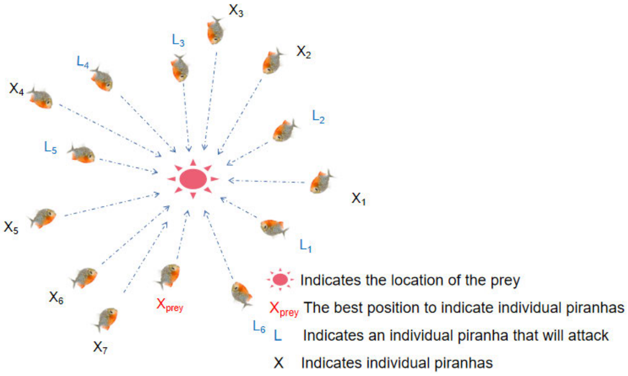
X_1
X_2
X_3
X_4
X_5
X_6
X_7
L_1
L_2
L_3
L_4
L_5
L_6
X_{prey}
Indicates the location of the prey
X_{prey} The best position to indicate individual piranhas
L Indicates an individual piranha that will attack
X Indicates individual piranhas

FIGURE 4. Schematic diagram of Localized Group Attack Pattern.

$$E = \begin{cases} 1 & \beta_3 \leq 0.5 \\ -1 & \beta_3 > 0.5 \end{cases} \tag{4}$$

where β_3 denotes a random number between 0 and 1.

STEP 5 Update the proxy location formula.

1) THE LOCALIZED GROUP ATTACK PATTERN

As a group foraging creature, it will attack prey several times larger than them when hungry. Whenever prey stray into their habitat, a splash of water is made and the keenly hearing piranha pick up this signal and quickly assemble to surround and bite the prey in turn, with the agent close to the prey being the first to attack, see Figure 4. The mathematical model of the localized group attack pattern is shown in Eq. (5).

$$x_i(t+1) = \gamma_1 \sum_{k=1}^{pc} \frac{L_k(t) - x_i(t)}{pc} - x_{prey}(t) \tag{5}$$

where $x_i(t+1)$ is the new location of the search agents, pc denotes a randomly generated integer in [6, SearchAgents_no/2], SearchAgents_no denotes the total number of agents, and $L_k(t)$ is the fraction of local population attacks that are performed to initiate the attack first, where $L \in X$, and X denotes the number of randomly generated piranhas. $x_i(t)$ denotes the current agent's position, $x_{prey}(t)$ denotes the location of the best agent found in the previous iteration, γ_1 is

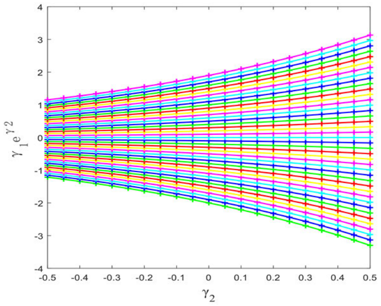

FIGURE 5. $\gamma_1 * e^{\gamma_2}$ **divergence curve chart.**

a random number uniformly distributed in [−2,2] which plays an important role in changing the trajectory of the piranha.

2) THE BLOODTHIRSTY CLUSTER ATTACK PATTERN

Piranhas have a special taste for and a keen awareness of the smell of blood, and when their prey is wounded and bleeding, it attracts distant piranhas to the area with a high concentration of blood to attack more aggressively. The higher the concentration of blood, the faster it swims. This stage relies heavily on the blood concentration F_i, the distance d_i between the piranhas and its prey and the non-linear cosine factor S, which is also influenced by E. Changing the direction of movement of the piranhas can effectively avoid local optima and enable it to find better prey locations, see Eq. (6).

$$x_i(t+1) = \gamma_1 * e^{\gamma_2} * x_{pery}(t) + G * x_{prey}(t) * E * F_i + E * \beta_4 * S * F_i \tag{6}$$

where $x_i(t+1)$ denotes the new location of the search agent, $x_{prey}(t)$ denotes the location of the best agent found in the previous iteration, γ_1 is a random number uniformly distributed in [−2, 2], γ_2 is a random number uniformly distributed in [−1/2, 1/2] and β_4 denotes a random number between 0 and 1. G is the coefficient of foraging ability of piranhas, taken as an integer of $G \geq 5$ ($G = 9$ is taken in this paper). $\gamma_1 * e^{\gamma_2}$ as shown in Figure 5 below, exhibits a uniform dispersion, allowing for dynamic adjustment and trade-offs between global and local search capabilities.

3) THE SCAVENGING FORAGING PATTERNS

During foraging, piranhas, because of their poor vision, break away from the group in turbid watersheds and at night, and swim randomly in their habitat as individuals, feeding on carrion and seeds, the modelling of Eq. (7). is shown in Figure 6 by vector analysis.

$$x_{i(t+1)} = \frac{1}{2}\left[e^{\gamma_2} * x_{C_1}(t) - E * x_i(t)\right] \tag{7}$$

where $x_i(t+1)$ denotes the new position of the search agent, γ_2 is a random number uniformly distributed in [−1,1], E is a parameter that changes the direction of movement, $x_{C_1}(t)$ denotes the c$_1$st agent position randomly selected from the piranhas, $x_i(t)$ denotes the i th agent position randomly selected from the agents, and $C_1 \neq i$.

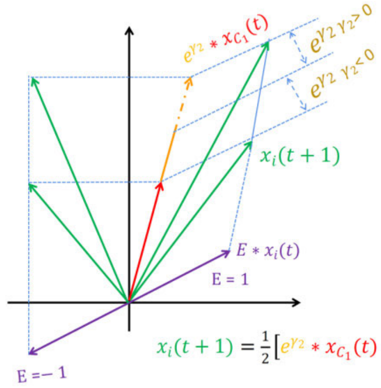
$e^{\gamma_2} * x_{C_1}(t)$
$e^{\gamma_2 \; \gamma_2>0}$
$e^{\gamma_2 \; \gamma_2<0}$
$x_i(t+1)$
$E * x_i(t)$
E = 1
E =− 1
$x_i(t+1) = \frac{1}{2}[e^{\gamma_2} * x_{C_1}(t) - E * x_i(t)]$

FIGURE 6. **Vector analysis of Eq. (7).**

4) THE PIRANHA POPULATION SURVIVAL STRATEGIES

The reproductive characteristics of piranhas and their numerous natural predators limit their population size. In order to maintain population diversity, the survival rate SR of the agent is first calculated using Eq. (8). and when the survival rate $SR \leq 1/4$ (i.e. low survival rate) the offspring population is reproduced by using Eq. (9).

$$SR(i) = \frac{fitness_{Max} - fitness(i)}{fitness_{Max} - fitness_{Min}} \tag{8}$$

$$x_i(t+1) = x_{prey}(t) + \frac{1}{2}\left\{\left[x_{C_1}(t) - E * x_{C_2}(t)\right] - \left[x_{C2}(t) - E * x_{C3}(t)\right]\right\} \tag{9}$$

where $x_i(t+1)$ denotes the new position of the search agent, $x_{prey}(t)$ denotes the position of the best agent found in the previous iteration, E is the parameter for changing the direction, and $x_{C_1}(t), x_{C_2}(t), x_{C_3}(t)$, denote the C_1, C_2, C_3 agent positions randomly selected from the piranhas with $C_1 \neq C_2 \neq C_3$ respectively. The PFOA pseudo-code is shown in Table 1. The flowchart for PFOA is shown in Figure 7.

C. ANALYSIS OF THE PFOA ALGORITHM

1) SENSITIVITY ANALYSIS OF MANUAL TUNING IN ALGORITHMS

This subsection is used to analyse the sensitivity of sets of custom parameters C & G in the PFOA algorithm, and the tested results are used in the third part of the experiments in this study.

a: SENSITIVITY ANALYSIS OF G & C IN PFOA

Since PFOA uses two user-defined parameters (G & C), it is important to select values for these parameters carefully because they affect PFOA performance significantly. To analyse the effect of these parameters on the performance of the PFOA, sensitivity tests were carried out using CEC Composition Function 2 ($N = 3$), see F24 in Table 5. CEC Composition Function 2 is composed of three basic functions ($N = 3$), G1: Rastrigin's F5, G2: Griewank's F15, G3: Modifed Schwefel's F10 functions are composed. As the test function contains multiple quadratic structures and is

TABLE 1. The pseudo-code of PFOA.

```
procedure PFOA
  Initialization of parameters
  M=0.5 is the probability that the piranha is hungry and the probability that it is in Attack Pattern or Scavenging Foraging Patterns
  N=0.75 is the probability of blood concentration in piranha habitat to determine whether a localized Group Attack Pattern or a Bloodthirsty Cluster Attack Pattern was carried out
  Generate the initial population
  while iteration < Max Number of iteration do
    if random < M then
      Update nonlinear cosine factor $S$, using Eq.(3).
        if random < N then
          Calculate the Blood Concentration Parameter $F_i$, using Eq.(2).
          Pattern 1 : localized Group Attack Pattern, using Eq.(5).
        else
          Pattern 2 : Bloodthirsty Cluster Attack Pattern, using Eq.(6).
        end if
  else
    Pattern 3 : Scavenging Foraging Patterns, using Eq.(7).
  end if
  Strategy 1: Piranha survival rate strategy, update formula when survival rate is low, using Eq.(8).
  Calculate $X_{new}$, the fitness value of the new search agents
  If $X_{new} < X_{prey}$ then
  Set $X_{prey} = X_{new}$
  end if
  Set iteration = iteration+1 end while Stop criteria satisfied
  Display $X_{prey}$ and the best optimal solution
  end procedure
```

TABLE 2. C & G sensitivity analysis of CEC Composition Function 2.

Param eters	Test 1	Test 2	Test 3	Test 4	Test 5
Tests	G = 1	G = 3	G = 6	G = 9	G = 12
C = 1	1.396E+04	1.287E+04	1.254E+04	1.113E+04	1.017E+04
C = 2	1.089E+04	1.132E+04	1.056E+04	9.667E+03	1.049E+04
C = 3	1.135E+04	1.041E+04	1.101E+04	1.012E+04	1.053E+04
C = 4	9.782E+03	9.372E+03	9.031E+03	8.322E+03	7.819E+03
C = 5	9.783E+03	9.158E+03	8.665E+03	**7.235E+03**	8.104E+03
C = 6	9.342E+03	8.426E+03	9.122E+03	8.262E+03	9.282E+03

highly non-linear and multi-peaked, the results of the test function are usually affected when the algorithm parameters are adjusted. CEC Composition Function 2 ($N = 3$) is often used to test the sensitivity of an algorithm to determine whether its performance is sufficiently robust to parameter changes.

The test experiment yielded five scenarios by combining different values of G and C. As it can be observed in Table 2 that for $G = 9$ the best fitness value was achieved at $C = 5$. This concludes that the best parameter values for the proposed algorithm are $G = 9$ and $C = 5$ (see Figure 8).

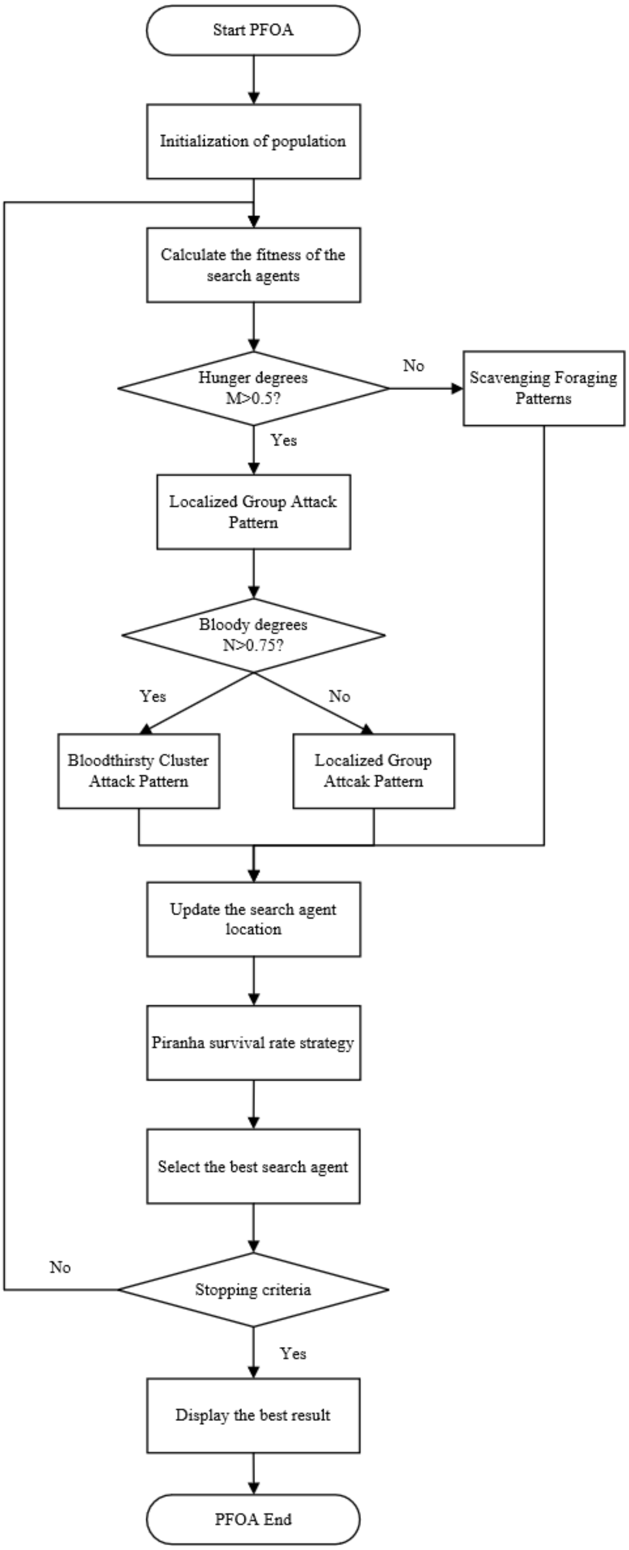
Start PFOA
Initialization of population
Calculate the fitness of the search agents
Hunger degrees M>0.5?
No
Scavenging Foraging Patterns
Yes
Localized Group Attack Pattern
Bloody degrees N>0.75?
Yes
No
Bloodthirsty Cluster Attack Pattern
Localized Group Attcak Pattern
Update the search agent location
Piranha survival rate strategy
Select the best search agent
No
Stopping criteria
Yes
Display the best result
PFOA End

FIGURE 7. The flowchart of PFOA.

b: POPULATION SIZE ANALYSIS OF PFOA

This subsection analyses the impact on search accuracy and convergence speed by testing the number of populations. The experiment fixed the number of iterations at 500, gradually

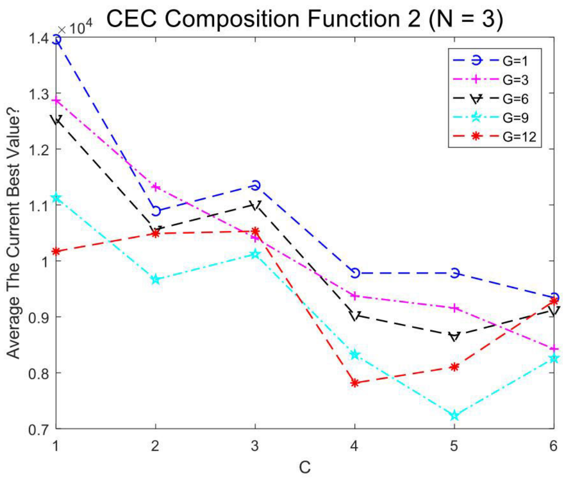

FIGURE 8. Fitness achieved by PFOA for parameters C & G.

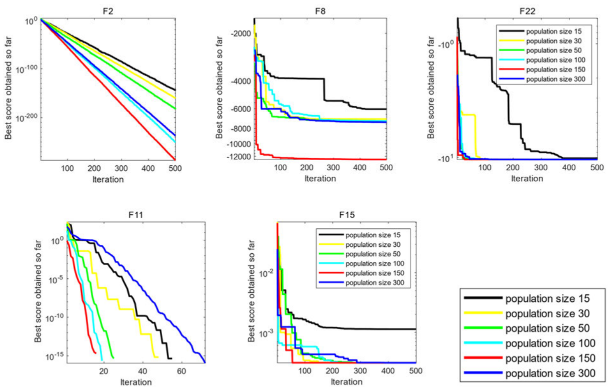

FIGURE 9. PFOA population size analysis.

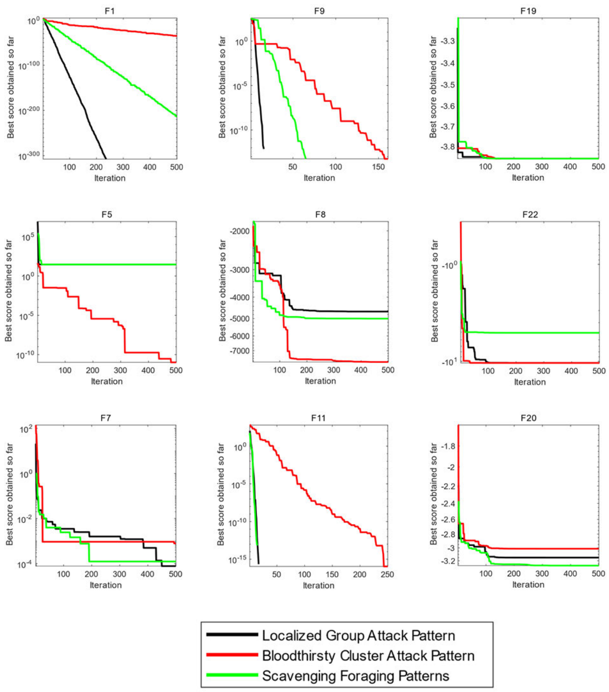

FIGURE 10. PFOA hunting patterns analysis.

increasing the population size by 15, 30, 50, 100, 150 and 300, and the comparative convergence curves are shown in Figure 9. By analyzing a partial suite of benchmark functions, PFOA algorithm achieves optimal performance when the population size is 150. In addition, the PFOA, with a population size of 30, continues to perform well when subsequently compared to other meta-heuristics.

c: ANALYSIS OF THE FORAGING PATTERNS OF PFOA

In order to better analyse the performance of each foraging pattern, three patterns of localized group attack, bloodthirsty cluster attack, and scavenging foraging were tested and studied separately for single-peaked, multi-peaked, and fixed-dimensional problems. This experiment is an improvement on the PFOA such that only one foraging mode is used for each run and eventually the convergence curves of several foraging modes are compared. In this test, the number of iterations was set to 500 and the population size (search agent) was set to 30. The output is shown in Figure 10, where the three foraging modes show their respective strengths under different benchmark function suite tests. Among them, the localized group attack pattern can quickly locate potential regions of prey and speed up the convergence of the algorithm. It performs best in the single-peaked function F1, the multi-peaked function F9 and the fixed-dimensional function F19. The bloodthirsty cluster attack pattern serves to accelerate the convergence of the algorithm in PFOA, performing well in the single-peaked function F5, the multi-peaked function F8 and the fixed-dimensional function F22, highlighting the advantages of its foraging mode convergence. The scavenging foraging pattern is the global search part of the algorithm and acts as a strict scan of the search area to avoid premature convergence of the algorithm. It also outperforms other foraging modes on the single-peaked function F7, the multi-peaked function F11 and the fixed-dimensional function F20.

d: TIME COMPLEXITY ANALYSIS OF PFOA

The computational complexity of the algorithm is an important criterion to measure the optimization time; according to the above pseudo codes, this paper uses big-O notation to represent the complexity [33]. The time complexity of PFOA is computed as follows.

For PFOA

1) Time complexity $O(N \times D)$ is consumed in the initial phase of the algorithm, where N is the number of piranha, and D is the dimension of the search space.

2) The fitness evaluation of each piranha requires $O(N)$ time.

3) The best position piranha selection costs $O(N)$ time.

4) The piranha position update of the original PFOA requires $O(N \times D)$ time.

In summary, the total computational time for the original PFOA is $O(N \times D \times M)$, where M is the maximum number of iterations.

III. EXPERIMENTS COMPARISON AND RESULTS

The numerical optimization efficiency of PFOA was verified by solving a suite of 27 benchmark functions and four engineering design problems. To test the performance of PFOA, we compared the experimental results with 13 meta-heuristic optimization. Among the improved classical algorithms used for comparison are: Fruit Fly Optimization Algorithm(FOA), Particle Swarm Optimization(PSO), Beetle Antennae Search(BAS) [34], Multi-population Invasive Weed Optimization(PMIWO) [35], Beetle antenna strategy based grey wolf optimization(BGWO), SHADE with Linear Population Reduction(L-SHADE) [36], Sparrow Search Algorithm Based on Lévy's Flight Perturbation Strategy(ISSA) [37]. The latest optimization algorithms for comparison are Dingo Optimization Algorithm(DOA), Chameleon Swarm Algorithm(CSA), Smell Agent Optimization(SAO), Honey Badger Algorithm(HBA), Chimp Optimization Algorithm(CHOA), Rat Swarm Optimization(RSO). On the one hand, among the algorithms chosen for comparison, such as FOA, PSO, BGWO, BAS, PMIWO, L-SHADE and ISSA are classical algorithms that are milestones in meta-heuristic optimization algorithms and their improvements. On the other hand, algorithms such as SAO, CSA, HBA, DOA and CHOA are the latest and better performing algorithms, which are very challenging to compare with and better highlight the performance characteristics of PFOA. The selection of these recognized and promising algorithms for comparison with our algorithm is sufficient to demonstrate the overall effectiveness of the proposed approach.

A. PARAMETERS AND HARDWARE SETTINGS IN THE EXPERIMENT

In addition to the algorithm-specific parameter settings mentioned in Table 3, the same parameters were used for both the PFOA and the competition algorithms in order to obtain a fairer comparison. The uniform settings include: hardware with MATLAB version R2018a, population size (search agents) set to 30 (SearchAgents_no), a maximum number of 1000 iterations (Max_iteration), and 30 independent runs for each optimization problem.

TABLE 3. The parameters setting of the comparison algorithm.

Algorithms	Parameters
FOA	pop=30 (Pop size)
PSO	SearchAgents_no=30 (Pop size) Inertia weight decreases linearly from 0.9 to 0.4 (Default) C_1 (individual-best acceleration factor) increases linearly from 0.5 to 2.5 (Default) C_2 (global-best acceleration factor) decreases linearly from 2.5 to 0.5 (Default)
BAS	pop=30 (Pop size) eta=0.95 c=5 (ratio between step and d_0) step=1 (initial step set as the largest input range)
BGWO	eta=0.95 c=5 (ratio between step and d_0) a = 2 (linearly decreased over iterations) step=1 (initial step set as the largest input range)

PMIWO	pop=30 (Pop size) nVar = 5 (Number of Decision Variables)
	VarSize = [1 nVar] (Decision Variables Matrix Size)
	Smin = 0 (Minimum Number of Seeds)
	Smax = 5 (Maximum Number of Seeds)
	Exponent = 2 (Variance Reduction Exponent)
	igma_initial = 0.5 (Initial Value of Standard Deviation)
	sigma_final = 0.001 (Final Value of Standard Deviation)

L-SHADE	N_{min}=4 H=100 $r_2 \in [1, H]$
ISSA	SearchAgents_no=30 (Pop size) $C_2 \in [0, 1]$ $C_3 \in [0, 1]$

SAO	SearchAgents_no=30 (Pop size) olf=0.9 K=0.6 T=0.95
	M=0.9
	Step=0.02

CSA	SearchAgents_no=30 (Pop size) p_1=0.25 p_2=1.5 ρ=1.0 c_1=1.75 c_2=1.75
HBA	Honey Badger number = 30 β(the honey badger to get food ability) = 6 C = 2

DOA	SearchAgents_no=30 (Pop size)
	P =0.5 (probability of hunting or scavenger strategy)
	Q=0.7 (probability of Strategy 1 (group attack) or Strategy 2 (persecution attack))

CHOA	SearchAgents_no=30 (Pop size) $f \in [0, 2.5]$ $a \in [-2f, 2f]$ $c \in [0, 2]$
RSO	SearchAgents_no=30 (Pop size) $R \in [1, 5]$ (Control parameter) $C \in [0, 2]$ (Constant Parameter)
PFOA	SearchAgents_no=30 (Pop size) M=0.5 (The probability of starvation in the habitat) N=0.75 (Blood taste concentration probability) C=5 (Constant Parameter) G=9 (Coefficient of foraging ability)

B. BENCHMARK FUNCTION SUITE ANALYSIS

1) DESCRIPTION OF THE BENCHMARK FUNCTION

The performance of PFOA is studied on a suite of 27 benchmark functions (CEC) [38] and compared with 13 state-of-the-art algorithms. The experiment is divided into four categories: the first is a single-peaked function (F1∼F7), which has only one global optimal solution and is mainly used to evaluate the development ability of intelligent optimization algorithms; the second multi-peaked function (F8∼F13) which has multiple local optimal regions and is mainly used to test the ability of intelligent optimization methods to jump out of the local optimum and find the global optimum. The third category is the fixed dimensional multi-peaked functions (F14 to F23), which have a large number of local optima and are used to test the ability to find the optimal value in a given dimension. The fourth category is the composite and hybrid functions (F24 to F27), which are highly complex and challenging and can effectively test the robustness of the algorithm. Due to their respective test characteristics, benchmark functions are often used to evaluate the comprehensive performance of meta-heuristics (which include rapidity, accuracy and stability of convergence). See Table 4-5 for details of the benchmark functions. In the table it is worth noting that *Dim* denotes the dimension of the benchmark function, *Interval* denotes the bound of the search space of the benchmark function, F_{min} denotes the value of the objective function at the optimal position and N means the number of functions available. In summary, 27 benchmark test functions of varying difficulty, which represent the most challenging optimization problems and are one of the most authoritative ways of verifying the performance of optimization algorithms, comprehensively test the performance of meta-heuristic optimization algorithms. We hope that these critical problems will effectively

TABLE 4. Introduction to 23 benchmarking functions (CEC).

Function	Name	Dimsion	Interval	F_{min}
$F_1(x)=\sum_{i=1}^{n} x_i^2$	Sphere	30/50/100	[−100, 100]	0
$F_2(x)=\sum_{i=1} \lvert x_i \rvert + \Pi_{i=1}^{n} \lvert x_i \rvert$	Schwefel’s 1.2	30/50/100	[−10, 10]	0
$F_3(x)=\sum_{i=1} \left(\sum_{j-1}^{i} x_j\right)^2$	Rotated Hyper-Ellipsoid	30/50/100	[−100, 100]	0
$F_4(x)=\max_i \{\lvert x_i \rvert, 1 \le i \le n\}$	Schwefel’s 2.21	30/50/100	[−100, 100]	0
$F_5(x)=\sum_{i=1}^{n-1} [100(x_{i+1}-x_i^2)^2+(x_i-1)^2$	Rosenbrock	30/50/100	[−30, 30]	0
$F_6(x)=\sum_{i=1}^{n} ([x_i+0.5])^2$	Step	30/50/100	[−100, 100]	0
$F_7(x)=\sum_{i=1}^{n} ix_i^4 + random[0,1)$	Griewangk	30/50/100	[−1.28, 1.28]	0
$F_8(x)=\sum_{i=1}^{n} -x_i \sin\left(\sqrt{\lvert x_i \rvert}\right)$	mvfSchwefel2_26	30/50/100	[−1000, 1000]	−418.9829 × d
$F_9(x)=\sum_{i=1}^{n} \left[x_i^2-10\cos(2\pi x_i+10)\right]$	mvfRastrigin	30/50/100	[−5.12, 5.12]	0
$F_{10}(x)=-20\,\boldsymbol{exp}\left(-0.2\sqrt{1/n \sum_{i=1}^{n} x_i^2}\right)-\boldsymbol{exp}\left(1/n \sum_{i=1}^{n} \boldsymbol{cos}(2\pi x_i)\right)+20+e$	Ackely	30/50/100	[−32, 32]	0
$F_{11}(x)=1/4000\sum_{i=1}^{n} x_i^2-\Pi_{i=1}^{n}\cos\left(\frac{x_i}{\sqrt{i}}\right)+1$	Griewangk 10	30/50/100	[−600, 600]	0
$F_{12}(x)=\pi/n\{10\sin(\pi y_1)+\sum_{i=1}^{n-1}(y_i-1)^2[1+10\sin^2(\pi y_{n+1})]+(y_n-1)^2\}$ $+\sum_{i=1}^{n} u(x_i,10,100,4)$	Alpine	30/50/100	[−50, 50]	0
$F_{13}(x)=0.1\{\sin^2(3\pi x_i)+\sum_{i=1}^{n}(x_i-1)^2[1+\sin^2(3\pi x_i+1)]+(x_n-1)^2$ $[1+\sin^2(2\pi x_n)]\}+\sum_{i=1}^{n} u(x_i,5,100,4)$	Griewangk	30/50/100	[−50, 50]	0
$F_{14}(x)=\left(1/500+\sum_{j=1}^{25} 1/j+\sum_{i=1}^{2}(x_i-a_{ij})^6\right)^{-1}$	De Jong’s (N.5)	2	[−65.536, 65.536]	0
$F_{15}(x)=\sum_{i=1}^{11}\left[a_i-x_1(b_i^2+b_i x_2)/b_i^2+b_i x_3+x_4\right]^2$	Kowalik	4	[−5, 5]	0.0003075
$F_{16}(x)=4x_1^2-2.1x_1^4+(1/3)x_1^6+x_1x_2-4x_2^2+42^4$	Trecanni	2	[−5, 5]	-1.0316285
$F_{17}(x)=(x_2-(5.1/4\pi^2)x_1^2+(5/\pi)x_1-6)^2+10(1-(1/8\pi))\cos x_1+10$	Branin	2	[−5, 5]	0.398
$F_{18}(x)=[1+(x_1+x_2+1)^2(19-14x_1+3x_1^2-14x_2+6x_1x_2+3x_2^2)]\times[30+(2x_1-3x_2)^2$ $\times(18-32x_1+12x_1^2+48x_2-36x_1x_2+27x_2^2)]$	Goldstein-Price	2	[-2, 2]	3
$F_{19}(x)=-\sum_{i=1}^{4} c_i\exp\left(-\sum_{j=1}^{3} a_{ij}(x_j-p_{ij})^2\right)$	Hartman	3	[1, 3]	-3.86
$F_{20}(x)=-\sum_{i=1}^{4} c_i\exp\left(-\sum_{j=1}^{6} a_{ij}(x_j-p_{ij})^2\right)$	Hartman	6	[0, 1]	-3.32
$F_{21}(x)=-\sum_{i=1}^{5}\left[(X-a_i)(X-a_i)^T+c_i\right]^{-1}$	Shekel foxholes	4	[0, 10]	-10.1532
$F_{22}(x)=-\sum_{i=1}^{7}\left[(X-a_i)(X-a_i)^T+c_i\right]^{-1}$	Shekel foxholes	4	[0, 10]	-10.402
$F_{23}(x)=-\sum_{i=1}^{10}\left[(X-a_i)(X-a_i)^T+c_i\right]^{-1}$	Shekel foxholes	4	[0, 10]	-10.536

TABLE 5. Basic parameters of the hybrid and composite test function(CEC).

	Composition Function	Name	F_{min}	Coverage(σ)	Defining the global optimum(bias)
F_{24}	G_1: Rastrigin’s F5 G_2: Griewank’s F15 G_3: Modifed Schwefel’s F10	Composition Function 2 (N=3)	4.0E+03	[10, 20, 30]	[0, 100, 200]
F_{25}	G_1: Ackley’s F13 G_2: High Conditioned Elliptic F11 G_3: Griewank’s F15 G_4:Rastrigin’s F5	Composition Function 4 (N=4)	3.5E+03	[10, 20, 30,40]	[0, 100, 200, 300]
	Hybrid Function	**Name**	**F_{min}**	**Function Occupancy Ratio**	
F_{26}	G_1:Zakharov’s F3 G_2:Rosenbrock’s F4 G_3:Rastrigin’s F5	Hybrid Function 1 (N=3)	0	P=[0.2, 0.4, 0.4]	
F_{27}	G_1:Bent Cigar’s F1 G_2:Rosenbrock’s F4 G_3:Lunache Bi-Rastrigin’s F7	Hybrid Function 4 (N=3)	0	P=[0.3, 0.3, 0.4]	

TABLE 6. Test data statistics for 27 benchmarking functions.

	ID	SAO	CSA	HBA	DOA	CHOA	RSO	PSO	FOA	BAS	MPIWO	BGWO	L-SHADE	ISSA	PFOA
	Best	6.7091E-05	4.0146E-03	1.1749E-291	0	6.5568E-25	0	6.6088E-02	1.8430E+04	1.5774E+00	4.9361E+01	6.0009E-61	4.9081E-168	5.4758E-09	**0**
F1	Mean	1.1193E-03	6.4664E-02	4.5005E-277	9.1889E-130	8.5140E-14	7.3108E-264	2.8062E-01	2.4053E+04	3.4907E+00	1.3046E+03	8.3440E-59	2.7816E-150	1.2357E-08	**0**
	STD	1.1766E-03	6.5707E-02	0	4.6854E-129	3.3167E-13	0	1.3084E-01	2.8724E+03	1.3576E+00	8.6261E+02	1.6522E-58	1.4094E-149	3.4438E-09	**0**
	Time	5.9999E-01	4.2241E-01	5.0021E-01	5.8781E-01	1.1534E+00	4.8467E-01	4.8677E-02	1.1665E-01	7.1783E-02	2.6824E-01	1.2377E-01	**4.8047E-02**	1.0775E-01	3.1635E-01
	Best	1.6763E-02	1.5403E+01	7.6185E-151	0	2.7637E-16	0	3.8970E-01	7.7904E+01	6.0250E-36	2.5959E-02	6.2385E-36	1.8795E-115	1.2764E-02	**0**
F2	Mean	1.1661E-01	5.8336E+00	1.1352E-146	6.2091E-64	2.7797E-10	3.7125E-284	9.9012E-01	1.0608E+05	9.1272E+00	4.0356E-02	8.8123E-35	2.3293E-103	8.8424E-01	**0**
	STD	8.9275E-02	2.2265E+00	1.7082E-146	3.3424E-83	9.5475E-10	0	4.7488E-01	3.1568E+05	1.4555E+00	4.3221E-02	7.6231E-35	9.7048E-103	1.0899E+00	**0**
	Time	9.3073E-02	5.6332E-01	5.1673E-01	5.8442E-01	1.1716E+00	5.8977E-01	**4.1119E-02**	1.2522E-01	6.5174E-02	2.6120E-01	1.2519E-01	4.9891E-02	1.0906E-01	3.0204E-01
	Best	7.4945E-03	4.3288E+02	1.3074E-220	0	2.0065E-06	0	4.3565E+01	3.3374E+04	5.2670E+00	2.4154E+04	1.0436E-19	2.7033E+03	3.9583E+01	**0**
F3	Mean	1.1554E+04	1.2756E+03	5.9218E-203	6.3557E-118	1.1358E+00	1.1577E-257	8.5155E+02	4.9796E+04	1.1062E+01	8.2444E+03	1.3742E-14	1.9133E+04	2.4641E+02	**0**
	STD	2.1838E+04	4.8799E+02	0	3.2408E-117	3.9026E+00	0	3.0954E+01	9.3161E+03	4.4170E+00	3.3849E+03	4.6578E-14	9.7710E+03	1.9359E+02	**0**
	Time	4.2473E-01	1.1297E-01	1.6495E-01	1.4346E-01	1.2251E+00	1.0997E-01	2.2178E-01	2.9323E-01	**2.3257E-02**	4.6606E-01	2.9180E-01	2.1449E-01	2.7476E-01	3.1050E-01
	Best	8.9608E-04	5.4338E+00	3.0031E-123	0	2.5361E-07	0	1.1707E+00	4.9808E+01	6.4309E-01	2.7698E+01	5.0367E-16	1.9113E-01	2.8056E+00	**0**
F4	Mean	5.2476E-02	1.1997E+01	2.8768E-116	3.8375E-216	3.0965E-03	3.8375E-217	1.6179E+00	5.3331E+01	9.0116E-01	3.7912E+01	1.9984E-14	3.8218E+01	8.0298E+01	**4.8196E-279**
	STD	2.3485E-01	2.9406E+00	1.5155E-115	0	5.3636E-03	0	2.2131E-01	1.5003E+00	9.4673E-02	5.4610E+00	2.9789E-14	2.7708E+01	3.3371E+00	**0**
	Time	9.2791E-01	5.4474E-01	7.8491E-01	5.8603E-01	1.1845E+00	5.7053E-01	5.2257E-02	1.2802E-01	7.8933E-02	2.4646E-01	1.2132E-01	4.5943E-02	1.0766E-01	**2.8721E-02**
	Best	2.7626E-04	2.8369E+01	1.9926E+01	2.8867E+01	2.8082E+01	2.8114E+01	1.1794E+02	1.4829E+07	1.6153E+02	2.5066E+01	2.6028E+01	2.6160E+01	2.5238E+01	**1.9244E-13**
F5	Mean	7.8457E-02	1.8078E+02	2.1787E+01	2.8926E+01	2.8854E+01	2.8729E+01	4.3281E+02	2.5933E+07	4.8753E+02	1.5794E+02	2.6878E+01	2.6999E+01	7.4168E+02	1.1638E+00
	STD	7.6025E-02	1.6125E+02	7.4096E-01	3.6731E-01	2.0002E-02	2.4369E-01	3.7266E+02	4.2169E+07	2.2476E+02	3.1026E+02	6.6722E-01	4.3090E-01	9.5390E+01	2.9991E+00
	Time	1.3733E-01	5.7233E-01	6.1872E-01	6.8553E-01	1.1722E+00	3.8987E-01	7.5000E-02	1.3935E-01	8.6167E-02	2.7344E-01	1.4415E-01	**7.0293E-02**	1.2789E-01	3.2549E-01
	Best	1.4852E-04	6.5855E-03	4.0203E-09	3.4767E+00	2.0182E+00	2.5461E+00	5.1135E-01	1.7933E+04	4.3298E+00	4.6121E-05	1.0861E-05	7.6532E-03	**8.1059E-09**	2.8705E-07
F6	Mean	1.5697E-03	1.0505E-01	6.5177E-08	5.5276E+00	3.1298E+00	3.5827E+00	2.3016E-01	2.3422E+04	7.3605E+00	1.1632E+03	5.4339E-01	8.0928E-02	1.2784E-08	2.5016E+00
	STD	1.8168E-03	1.6759E-01	1.0250E-07	9.7105E-01	4.1473E-01	5.4944E-01	2.0078E-01	2.7485E+03	1.9762E-01	9.4721E+02	3.0744E-01	9.1246E-02	2.5844E-09	2.1651E+00
	Time	8.9203E-02	7.5307E-02	7.9733E-02	5.4531E-02	1.1493E+00	**2.6681E-02**	4.8807E-02	1.1457E-01	6.1897E-02	2.6053E-01	1.2257E-01	4.6903E-02	1.0935E-01	3.0244E-01
	Best	1.9018E-03	2.2860E-01	8.1385E-06	1.4609E-05	5.8663E-05	3.3357E-06	2.3330E-01	6.3537E+00	1.1900E-03	1.2624E-02	2.5365E-04	9.5823E-06	4.2051E-02	**2.9570E-06**
F7	Mean	1.1885E-02	7.0832E-01	1.6902E-04	2.4076E-04	1.0384E-03	2.4590E-04	3.0356E+00	1.4329E+01	2.8448E-02	2.6538E-02	8.6216E-04	1.8891E-03	9.0943E-01	5.4959E-05
	STD	1.1296E-02	2.3572E-01	1.4431E-04	2.8426E-04	1.2968E-03	2.5358E-04	2.8917E+00	2.8561E+00	1.2837E-02	7.1499E-02	3.8923E-04	1.8149E-03	3.4954E-02	5.2186E-05
	Time	2.9308E-01	**7.7683E-02**	1.3290E-01	1.1174E-01	1.2107E+00	7.9823E-02	1.5349E-01	2.1648E-01	1.7847E-01	3.9703E-01	2.2293E-01	1.5157E-01	2.0663E-01	3.5897E-01
	Best	-1.0573E+04	-1.2569E+04	-1.1049E+04	-7.0578E+03	-5.9266E+03	-7.7148E+03	-8.2068E+03	-7.5564E+03	-6.1745E+03	-7.9930E+03	-7.4588E+03	**-1.2569E+04**	-9.0821E+03	-1.2462E+04
F8	Mean	-5.0782E+03	-7.4768E+03	-7.4768E+03	-4.7877E+03	-5.7608E+03	5.7974E+03	-6.7264E+03	-6.9433E+03	-4.5322E+03	-6.4980E+03	-5.6998E+03	-1.0433E+04	-7.6757E+03	-7.1582E+03
	STD	2.7258E+03	2.5437E+03	2.5437E+03	8.2081E+02	6.5626E+01	1.1922E+03	7.7945E+02	3.7024E+02	7.3542E+02	7.0509E+02	8.7424E+02	1.6129E+03	8.2698E+02	2.2712E+03
	Time	1.3862E-01	4.6713E-01	6.2571E-01	6.9803E-01	1.1641E+00	4.7991E-01	8.5791E-02	1.4311E-01	**7.1487E-02**	2.8432E-01	1.5079E-01	7.3797E-02	1.3158E-01	3.1209E-01
	Best	5.2741E-03	1.4925E+01	0	0	2.8422E-13	0	5.7720E+01	2.7025E+02	6.6308E+01	4.7767E+01	0	0	2.3879E+01	**0**
F9	Mean	4.3348E+00	3.3931E+01	0	0	5.0237E+01	0	1.1234E+02	3.1243E+02	1.0162E+02	7.7649E+01	1.5158E-14	0	5.7708E+01	**0**
	STD	1.0081E+01	1.1665E+01	0	0	7.7351E+01	0	2.8490E+01	1.6995E+00	1.8567E+01	1.6822E+01	2.5137E-14	0	1.8114E+01	**0**
	Time	4.2993E-01	4.1512E-01	5.1772E-01	6.2323E-01	1.2092E+00	4.2177E-01	**7.0041E-02**	1.3912E-01	7.5233E-02	2.5144E-01	1.2742E-01	7.3513E-02	1.2256E-01	3.0596E-01
	Best	3.8878E-03	1.9967E+01	8.8818E-16	8.8818E-16	1.9960E+01	8.8818E-16	2.5630E-01	1.7078E+01	5.6187E-01	1.7258E+01	7.9048E-14	8.8818E-16	2.3876E-05	**8.8818E-16**
F10	Mean	1.6672E-02	1.9967E+01	1.4921E+00	1.0066E-15	1.9962E+01	1.0066E-15	9.1139E-01	1.8470E+01	1.7541E+00	1.8996E+01	1.0558E-13	3.9672E-15	2.2078E+00	**8.8818E-16**
	STD	9.7525E-03	3.7019E-13	5.7764E+00	6.3773E-16	1.1865E-03	6.3773E-16	5.1780E-01	5.3365E-01	5.0643E-01	4.2753E-01	1.9236E-14	2.3803E-15	6.6271E-01	**0**
	Time	4.3886E-01	4.7791E-01	4.6247E-01	6.1412E-01	1.1720E+00	5.3277E-01	7.0170E-02	1.4566E-01	7.8471E-02	2.4247E-01	1.2959E-01	7.8693E-02	1.2889E-01	**3.0519E-02**
	Best	3.6164E-06	1.1546E-01	0	0	0	0	3.2204E-03	1.5616E+02	8.0746E-01	4.2147E+02	0	0	5.7111E-08	**0**
F11	Mean	9.6307E-01	6.5406E-01	0	0	9.1360E-03	0	2.2087E-02	2.1246E+02	1.7618E-01	4.9576E+02	2.0707E-03	1.4527E-02	1.2146E-02	**0**
	STD	3.4158E+00	2.7778E-01	0	0	1.7248E-02	0	1.4826E-02	2.4588E+01	5.9139E-02	3.8235E+01	5.8420E-03	4.7621E-02	1.3267E-02	**0**
	Time	4.6114E-01	4.2997E-01	5.2793E-01	6.8921E-01	1.1670E+00	4.3251E-01	**8.1873E-02**	1.5902E-01	9.0533E-02	3.1471E-01	1.4721E-01	9.2321E-02	1.4261E-01	3.1628E-01
	Best	2.3736E-06	2.4748E+00	4.1797E-10	2.4737E-01	1.6730E-01	1.6292E-01	7.6784E-04	7.6626E+06	1.8285E-01	1.2241E+01	1.3702E-02	1.1151E-02	1.7435E+00	**6.7213E-15**
F12	Mean	6.7672E+00	6.3159E+00	3.5865E-08	5.7147E-01	3.9673E-01	3.4031E-01	9.9712E-03	1.3010E+07	4.7304E-01	2.0339E+01	4.8001E-02	7.3852E-03	5.8380E+00	5.6799E-01
	STD	2.0044E+01	2.0379E+00	1.1871E-07	1.9481E-01	1.9411E-01	1.0253E-02	2.6099E-02	2.3127E+06	1.5459E-01	6.5399E+00	2.3255E-02	8.8212E-03	3.4080E+00	3.3146E-01
	Time	6.5007E-01	4.6338E-01	5.1872E-01	4.9857E-01	1.2960E+00	4.6607E-01	3.7607E-01	3.9623E-01	**3.5227E-02**	5.7877E-01	3.9159E-01	3.1947E-01	3.8109E-01	4.3964E-01
	Best	2.5946E-05	2.6859E+01	8.4268E-08	2.2052E+00	2.6021E+00	2.7388E+00	2.7335E-02	3.3051E+07	2.2889E+00	6.6673E-06	1.9781E-01	2.5831E-02	9.4990E-10	**3.0514E-26**
F13	Mean	1.0601E-01	4.8921E+01	9.2167E-02	2.9198E+00	2.8385E+00	2.8419E+00	1.0086E-01	6.4077E+07	4.3809E+00	7.4213E-04	5.3842E-01	2.4016E-01	1.7674E+00	5.7760E-02
	STD	5.6916E-01	2.5146E+01	1.1152E-01	3.0330E-01	1.1934E-01	4.7903E-02	6.2047E-02	1.0604E+07	9.7285E-01	2.7417E-03	1.5489E-01	2.1777E-01	5.9406E+00	1.7438E-01
	Time	6.5894E-01	4.6682E-01	5.1881E-01	4.9418E-01	1.3007E+00	4.6471E-01	3.3235E-01	3.9942E-01	3.5243E-01	5.9351E-01	3.9481E-01	3.2381E-01	3.8276E-01	**3.3163E-01**
	Best	9.9800E-01	9.9800E-01	9.9800E-01	9.9800E-01	9.9800E-01	9.9800E-01	9.9800E-01	9.9800E-01	9.9800E-01	9.9800E-01	9.9800E-01	9.9800E-01	9.9800E-01	9.9800E-01
F14	Mean	5.1647E+00	1.0311E+00	1.1965E+00	3.2298E+00	9.9802E+00	2.4758E+00	2.3510E+00	9.9801E-01	**9.9800E-01**	1.1142E+01	4.2250E+00	2.7961E+00	1.1629E+00	1.5676E+00
	STD	4.8732E+00	1.7843E-01	5.3749E-01	2.7776E+00	3.1757E-05	2.4044E+00	1.4942E+00	1.9140E-07	**0**	6.9598E+00	4.3385E+00	3.2300E+00	7.2560E-01	1.1289E+00
	Time	1.0161E+00	4.5816E-01	5.8690E-01	4.8949E-01	5.3868E-01	4.5851E-01	4.9991E-01	5.7559E-01	**5.6861E-02**	1.4030E+00	5.7682E-01	5.1668E-01	5.5328E-01	4.1035E-01
	Best	4.7185E-04	3.0749E-04	3.0749E-04	3.0749E-04	1.2275E-03	3.5985E-04	6.8842E-04	1.2676E-03	1.2424E-03	3.0749E-04	3.0749E-04	3.0827E-04	5.0501E-04	3.0749E-04
F15	Mean	4.4822E-03	**1.2479E-03**	4.0574E-03	2.1029E-03	1.2823E-03	8.1674E-04	8.7532E-04	1.8815E-03	2.8753E-02	5.3300E-03	3.0129E-03	6.1015E-04	7.9505E-04	3.9451E-03
	STD	7.9421E-02	3.5670E-03	7.5228E-03	5.2364E-03	3.7486E-05	3.6335E-04	1.0021E-04	3.6951E-04	3.4988E-02	8.3001E-03	6.8074E-03	2.7742E-04	1.8582E-04	7.7516E-03
	Time	7.1813E-02	6.9831E-02	5.6363E-02	5.6057E-02	1.7487E-01	4.8381E-02	**2.3680E-02**	9.5731E-02	6.5787E-02	3.1203E-01	5.0547E-02	4.1717E-02	7.9843E-02	2.7711E-01
	Best	-1.0316E+00	-1.0316E+00	-1.0316E+00	-1.0316E+00	-1.0316E+00	-1.0316E+00	-1.0316E+00	-1.0316E+00	-1.0316E+00	-1.0316E+00	-1.0316E+00	-1.0316E+00	-1.0316E+00	**-1.0316E+00**
F16	Mean	-1.0316E+00	-1.0316E+00	-1.0316E+00	-1.0316E+00	-1.0316E+00	-1.0315E+00	-1.0316E+00	-1.0311E+00	-9.3611E-01	-1.0316E+00	-1.0316E+00	-1.0316E+00	-1.0316E+00	**-1.0316E+00**
	STD	1.5787E-05	0	0	0	7.4326E-06	1.1347E-04	0	4.9339E-04	2.3633E-01	4.2382E-09	6.3392E-09	6.8465E-11	1.3727E-14	**0**
	Time	7.3787E-02	6.2883E-02	5.3393E-02	5.2963E-02	9.7631E-02	5.9221E-02	3.7438E-02	9.4361E-02	6.8112E-02	3.9423E-01	4.3723E-02	4.4013E-02	7.8903E-02	**3.6489E-02**
	Best	3.9789E-01	3.9789E-01	3.9789E-01	3.9789E-01	3.9790E-01	4.0951E-01	3.9789E-01	3.9789E-01	3.9789E-01	3.9789E-01	3.9789E-01	3.9789E-01	3.9789E-01	**3.9789E-01**
F17	Mean	4.3108E-01	3.9789E-01	3.9789E-01	3.9789E-01	3.9824E-01	1.3010E+00	3.9789E-01	3.9800E-01	3.9789E-01	3.9789E-01	3.9789E-01	3.9789E-01	3.9789E-01	**3.9789E-01**
	STD	8.6694E-02	0	0	1.4055E-06	4.5362E-04	1.0128E+00	0	1.2365E-04	3.3445E-16	2.0947E-09	7.6750E-07	3.6554E-06	1.5150E-14	**0**
	Time	5.7241E-01	5.8477E-01	5.1791E-01	5.3631E-01	9.3541E-01	5.5567E-01	1.6397E-02	8.7203E-02	**5.9431E-03**	3.7269E-01	3.5037E-02	3.5651E-02	6.9781E-02	2.7839E-01
	Best	3.0000E+00	3.0000E+00	3.0000E+00	3.0000E+00	3.0000E+00	3.0000E+00	3.0000E+00	3.0002E+00	3.0000E+00	3.0000E+00	3.0000E+00	3.0000E+00	3.0000E+00	**3.0000E+00**
F18	Mean	3.0573E+00	3.0000E+00	5.7000E+00	3.0002E+00	3.0000E+00	3.0000E+00	3.0000E+00	3.0028E+00	1.1630E+01	3.0000E+00	3.0000E+00	3.0000E+00	3.0000E+00	**3.0000E+00**
	STD	1.9769E-01	0	1.4540E+01	1.0087E-03	7.8339E-05	2.6995E-05	3.2432E-15	2.4141E-03	2.1615E+01	2.9507E-07	1.6656E-05	1.5557E-05	9.7484E-14	**0**
	Time	5.3923E-01	5.8163E-01	5.9267E-01	5.2541E-01	9.2243E-01	5.4011E-01	1.4451E-02	8.6162E-02	**5.7665E-03**	3.7693E-01	3.5637E-02	3.1321E-01	6.8903E-02	2.6414E-01
	Best	-3.8628E+00	-3.8628E+00	-3.8628E+00	-3.8628E+00	-3.8612E+00	-3.8187E+00	-3.8628E+00	-3.8626E+00	-3.8628E+00	-3.8628E+00	-3.8628E+00	-3.8628E+00	-3.8628E+00	-3.8628E+00
F19	Mean	-3.8420E+00	-3.8628E+00	-3.8617E+00	-3.8611E+00	-3.8551E+00	-3.4841E+00	-3.8628E+00	-3.8614E+00	-3.4109E+00	-3.8628E+00	-3.8622E+00	-3.8611E+00	-3.8628E+00	-3.8628E+00
	STD	2.6799E-02	2.6645E-15	2.6792E-03	7.6955E-03	1.6495E-03	2.6224E-01	2.6645E-15	7.2564E-04	6.1392E-01	1.7962E-07	1.6269E-03	2.2322E-03	3.2387E-14	**1.3714E-15**
	Time	9.2867E-02	8.5693E-02	6.77987E-02	5.7987E-02	1.4118E-01	5.2811E-02	**2.9357E-02**	1.0240E-01	7.2371E-02	3.5341E-01	5.5807E-02	4.8667E-02	8.4273E-02	2.7720E-01
	Best	-3.0605E+00	-3.3220E+00	-3.3220E+00	-3.3220E+00	-3.0757E+00	-2.6346E+00	-3.3220E+00	-3.3128E+00	-3.3220E+00	-3.2031E+00	-3.3220E+00	-3.3220E+00	-3.3220E+00	-3.3220E+00
F20	Mean	-2.9640E+00	-3.2702E+00	-3.2500E+00	-3.2461E+00	-2.5751E+00	-1.6785E+00	-3.2784E+00	-3.2768E+00	-3.2733E+00	-3.2031E+00	-3.2918E+00	-3.2789E+00	-3.2370E+00	-3.1230E+00
	STD	3.9574E-01	5.9190E-02	8.2719E-02	8.3425E-02	3.7323E-01	4.3149E-01	5.7294E-02	5.3914E-02	9.6350E-02	1.3505E-05	6.3596E-02	1.0044E-01	5.5747E-02	**4.3969E-02**
	Time	4.7497E-01	4.6523E-01	5.2241E-01	5.9297E-01	5.5631E-01	4.3643E-01	3.4271E-02	1.0668E-01	**7.3276E-03**	2.8759E-01	6.3543E-02	4.9713E-02	8.9323E-02	2.8437E-01
	Best	-1.0153E+01	-1.0153E+01	-1.0153E+01	-1.0153E+01	-5.0394E+00	-2.7064E+00	-1.0153E+01	-9.8384E+00	-5.0552E+00	-1.0153E+01	-1.0153E+01	-1.0153E+01	-1.0153E+01	-1.0153E+01
F21	Mean	-8.5423E+00	-8.8904E+00	-9.6517E+00	-7.4311E+00	-3.1493E+00	-8.0167E-01	-8.3616E+00	-8.5516E+00	-5.0552E+00	-5.1481E+00	-9.4776E+00	-8.6196E+00	-7.5526E+00	**-9.9549E+00**
	STD	2.4703E+00	2.3265E+00	1.8765E+00	3.0868E+00	2.1160E+00	4.9991E-01	2.7978E+00	6.2132E-01	0	3.1582E+00	1.7213E+00	2.3359E+00	3.0748E+00	6.9981E-01
	Time	4.6509E-01	4.0763E-01	4.0759E-01	4.0707E-01	4.2287E-01	6.6813E-01	**1.2499E-01**	1.9592E-01	1.6322E-01	4.5097E-01	1.4563E-01	1.3866E-01	1.8248E-01	3.2994E-01
	Best	-1.0402E+01	-1.0403E+01	-1.0403E+01	-1.0403E+01	-5.0640E+00	-2.9910E+00	-1.0403E+01	-1.0055E+01	-5.0877E+00	-1.0403E+01	-1.0402E+01	-1.0403E+01	-1.0403E+01	-1.0403E+01
F22	Mean	-8.1055E+00	-9.5225E+00	-9.4496E+00	-8.5275E+00	-3.4967E+00	-1.0720E+00	-9.6226E+00	-8.7135E+00	-5.0877E+00	-7.4652E+00	**-1.0049E+01**	-9.0000E+00	-8.9825E+00	-9.8885E+00
	STD	2.8249E+00	1.9686E+00	2.4489E+00	2.9232E+00	1.9962E+00	6.6992E-01	2.0194E+00	6.8454E-01	0	3.4275E+00	1.3207E+00	2.5913E+00	2.6500E+00	1.6064E+00
	Time	5.4715E-01	4.3631E-01	5.2793E-01	4.2498E-01	4.4681E-01	8.9491E-01	1.6347E-01	2.3195E-01	**2.1711E-02**	4.9001E-01	1.8801E-01	1.8013E-01	2.2014E-01	3.4269E-01
	Best	-1.0535E+01	-1.0536E+01	-1.0536E+01	-1.0536E+01	-5.1030E+00	-2.7873E+00	-1.0536E+01	-1.0196E+01	-5.1285E+00	-1.0536E+01	-1.0536E+01	-1.0536E+01	-1.0536E+01	-1.0536E+01
F23	Mean	-8.1322E+00	**-1.0358E+01**	-8.574E+00	-8.466E+00	-3.8219E+00	-1.1205E+00	-9.6413E+00	-8.7683E+00	-5.1285E+00	-5.8321E+00	-1.0085E+01	-9.2826E+00	-9.6368E+00	-9.9870E+00
	STD	2.8391E+00	9.6229E-01	3.2722E+00	2.9973E+00	1.8825E+00	5.6884E-01	2.0014E+00	7.1989E-01	3.2432E+00	3.6901E+00	1.7223E+00	2.5391E+00	2.3468E+00	1.6416E+00
	Time	4.6483E-01	4.1858E-01	4.5907E-01	4.5596E-01	4.7269E-01	4.1776E-01	**2.2349E-02**	2.9693E-01	2.5887E-02	5.8936E-01	2.4849E-01	2.3854E-01	2.7607E-01	3.7859E-01
	Best	1.2365E+04	1.2569E+04	1.1521E+04	6.3789E+03	5.9153E+03	7.0226E+03	1.2548E+04	7.5927E+03	9.2548E+03	7.6275E+03	7.5340E+03	1.2568E+04	9.1544E+03	**4.235E+03**
F24	Mean	5.3464E+03	7.6187E+03	8.6002E+03	4.6894E+03	5.7653E+03	5.9676E+03	5.7340E+03	6.9347E+03	5.3459E+03	6.6846E+03	6.2903E+03	1.1166E+04	7.7006E+03	4.893E+03
	STD	3.2226E+03	2.6195E+03	1.5392E+03	8.4539E+02	5.8556E+01	6.6919E+02	2.7593E+03	3.3882E+02	4.5281E+02	5.0386E+02	8.4453E+02	1.4473E+03	6.1564E+03	3.1505E+03
	Time	2.9220E-01	7.9187E-02	1.2482E-01	1.2037E-01	8.3444E-01	5.7884E-02	6.9371E-02	1.4024E-01	6.6867E-02	**2.5838E-02**	7.5020E-02	5.7302E-02	1.2275E-01	4.8712E-02
	Best	1.6049E+54	1.6162E+61	6.7317E+04	8.0976E+04	8.2278E+04	8.2107E+04	1.2390E+61	6.1969E+58	7.8370E+04.	2.0938E+61	**4.5974E+03**	7.1322E+04	1.6309E+34	1.8067E+04
F25	Mean	2.8994E+58	5.3133E+26	3.2884E+16	8.9641E+14	1.5869E+19	8.5254E+16	4.8801E+61	1.9228E+59	8448E+02	6.8930E+61	1.1571E+23	1.5743E+18	1.0663E+35	4.6532E+16
	STD	4.9771E+58	2.4292E+61	1.7709E+17	2.0472E+14	8.1260E+19	3.0112E+16	2.2981E+61	6.8376E+58	2.0816E+02	3.6282E+61	2.8211E+23	8.4781E+18	8.8814E+34	7.7552E+16
	Time	3.2285E-01	8.3512E-02	1.2877E-01	1.1850E-01	8.3661E-01	6.1477E-02	8.0635E-02	1.4996E-01	**6.5763E-03**	3.1425E-01	7.8518E-02	5.6763E-02	1.2728E-01	1.2541E-01
	Best	2.8533E+21	6.8941E+28	3.8253E-01	9.4555E+00	7.6911E+00	8.7992E+00	1.0607E+29	5.5018E+00	7.1305E+00	1.9706E+29	5.5018E+00	6.0180E+00	3.0841E+06	**2.3581E-01**
F26	Mean	2.3179E+26	3.9341E+29	3.2950E-01	9.8470E+00	5.4786E+01	9.2395E+00	4.2804E+29	1.1162E+07	2.7244E+01	6.5241E+29	1.1162E+07	2.3167E+05	4.8334E+14	7.1853E-02
	STD	5.6540E+26	1.8189E+29	1.3484E+00	1.0840E-01	2.4181E+02	4.1528E-01	1.9604E+29	5.7860E+07	1.7944E+01	2.5351E+29	5.7860E+07	9.1432E+05	1.6045E+15	5.2328E-01
	Time	4.2131E-01	1.1570E-01	1.3051E-01	1.1527E-01	1.4359E+00	6.0261E-02	1.0408E-01	1.7514E-01	6.4207E-03	3.3971E-01	7.1411E-02	4.8217E-02	1.2352E-01	**5.1463E-02**
	Best	9.1941E+235	3.577E+259	1.8377E-150	0	2.4422E-11	0	4.214E+259	2.371E+255	1.9031E-01	1.947E+261	6.8604E-39	1.8890E-93	1.7455E+233	**0**
F27	Mean	1.3804E+215	5.905E+262	2.5533E-141	1.0718E-19	1.0414E-01	1.5194E-259	7.558E+262	9.794E+257	1.2025E+00	1.452E+264	2.3549E-35	5.0889E-82	1.0413E+250	0
	STD	-	-	1.3676E-140	5.7720E-19	5.0428E-02	0	-	-	5.7610E-01	-	7.3548E-35	1.9035E-81	-	0
	Time	2.0425E-01	5.8343E-02	1.1871E-01	1.1094E-01	8.1344E-01	4.6473E-02	4.7681E-02	1.1511E-01	**6.2516E-03**	2.7032E-01	6.5616E-02	4.3570E-02	1.0058E-01	3.5637E-02

validate the performance of PFOA and other optimization algorithms.

2) BENCHMARK FUNCTION SUITE TEST RESULT STATISTICS

This subsection carries out the statistics of the test results of the selected comparison algorithms on the 27 standard test functions. To make the experiment more convincing, Table 6 shows the best fit values (Best), the mean (Mean), standard deviation (STD) and run time (Time) of the best fit for the selected algorithm over 30 independent runs. Based on the data in the table 6, it can be seen that PFOA performs well in the vast majority of the 27 tested functions, with this

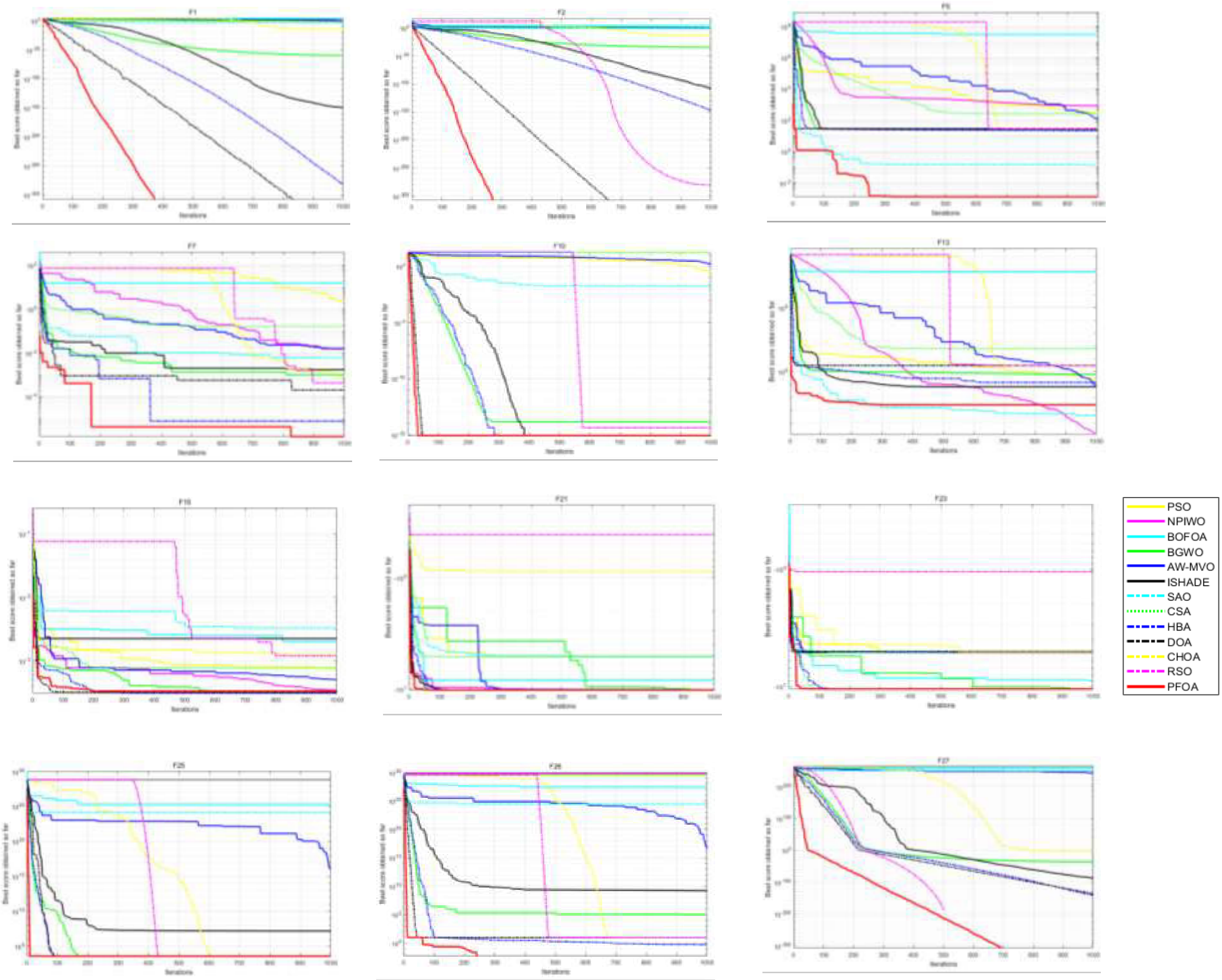

FIGURE 11. Comparison of challenging algorithms with PFOA.

algorithm having a clear advantage in difficult optimization problems such as F5, F7, F12, F13,F24 and F26, reaching an absolute global optimum level. For some of the functions tested, multiple algorithms are able to reach their theoretical optimal values and are strong rivals to PFOA, when comparing the mean and standard deviation is one of the effective means of comparing the advantages and disadvantages. PFOA's F1-F4, F10 and F19-F21 achieved theoretical optimums and a high level of algorithm stability. Just because there is no end to optimization, this algorithm is not optimal in e.g. F6, F8, F14, F23, F25 test functions, which is the goal of future research on this algorithm.

3) CONVERGENCE ANALYSIS

The PFOA statistical results discussed earlier confirm its robustness. In order to further compare The efficiency of the search process of the various algorithms in the optimization process, a comparative convergence figure of the algorithms is plotted in this paper, see Figure 11. It is observed from the graphs that the test functions F1-F5, F7, F9-F11, F21, F25 and F26 PFOA is significantly faster than FOA, PSO, BAS, PMIWO, ISSA, SAO, CSA, CHOA, RSO. The figure it can also be seen that FOA, PSO, BAS, PMIWO, ISSA, CSA, CHOA do not show any improvement for most of the search process as they are forced to converge prematurely due to being Trapped in local optima.In this experimental study, Overall, the convergence analysis in this section shows that the PFOA algorithm proposed in this paper is still the best among all the methods, and it is able to find the global optimum position faster than other methods.

4) BOX LINE CHART ANALYSIS

Also, to investigate the distribution characteristics of the solutions of the PFOA and comparison algorithms in solving the 27 benchmark functions, the results of 30 consecutive independent runs were plotted as box plots [39], as in Figure 12. Compared to its competitors, the PFOA proposed in this paper performs well for most functions F1, F3, F6, F7, F9, F10-F12 and F25, and the median, maximum and minimum

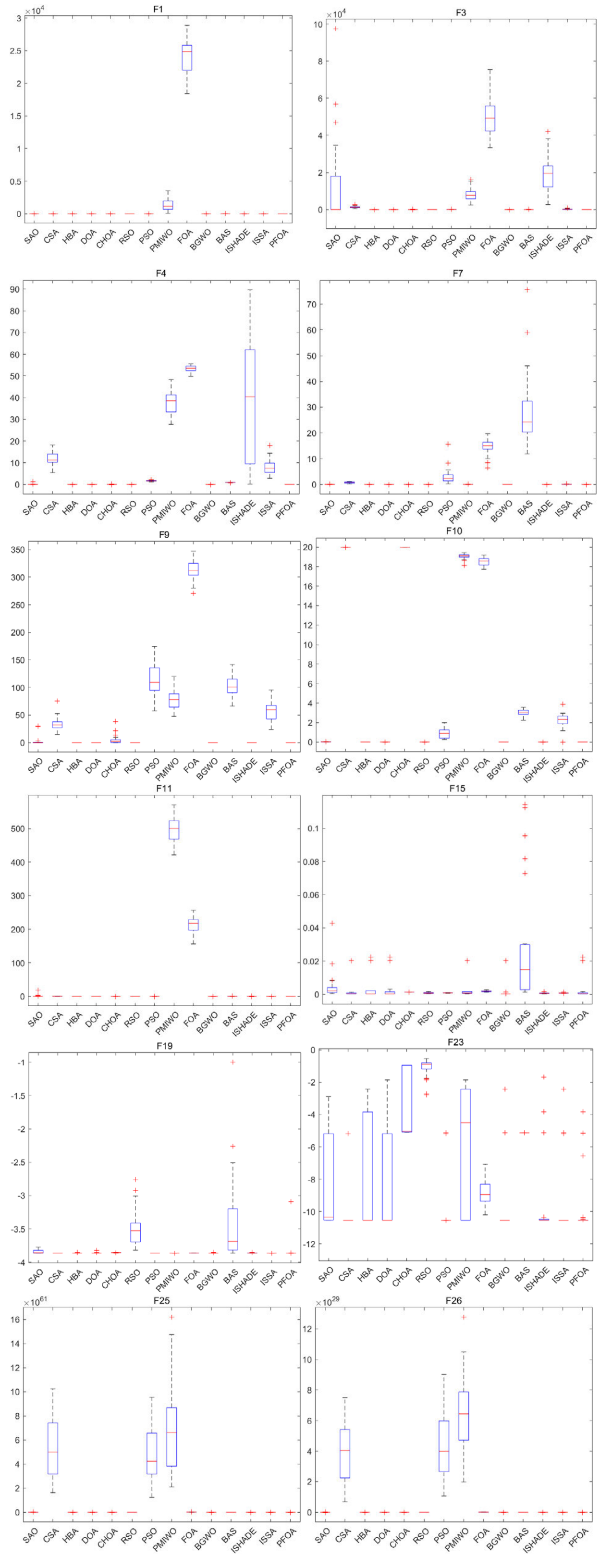

FIGURE 12. Box plot analysis for benchmark functions (Dim = 30).

values of this algorithm are almost identical to the optimal solution. However, individual test functions still have shortcomings, such as F8, F14 and other parts of the test functions have problems with large fluctuations. In summary, analysis of the vast majority of convergence curves and box plots shows that PFOA has greater optimization power and better stability than other algorithms, making it an optimizer with excellent performance in solving global optimization problems.

TABLE 7. Wilcoxon's rank sum test statistical results.

PFOA VS.		F1-F13 Dim=30	F1-F13 Dim=50	F1-F13 Dim=100	F14-F23 Fixed-Dim
Wilcoxon's rank sum test (+/ = /-)	SAO	(11/ 0 /2)	(12/ 0 /1)	(13/ 0 /0)	(13/ 0 /0)
	CSA	(13/ 0 /0)	(13/ 0 /0)	(13/ 0 /0)	(9/ 2 /2)
	HBA	(10/ 2 /1)	(9/ 2 /2)	(9/ 2 /2)	(9/ 2 /2)
	DOA	(10/ 2 /1)	(9/ 3 /1)	(11/ 1 /1)	(10/ 2 /1)
	CHOA	(12/ 0 /1)	(13/ 0 /0)	(13/ 0 /0)	(13/ 0 /0)
	RSO	(6/ 2 /5)	(8/ 2 /3)	(9/ 1 /3)	(12/ 0 /1)
	PSO	(12/ 0 /1)	(13/ 0 /0)	(13/ 0 /0)	(12/ 0 /1)
	BAS	(12/ 0 /1)	(13/ 0 /0)	(13/ 0 /0)	(12/ 0 /1)
	FOA	(13/ 0 /0)	(12/ 0 /1)	(12/ 0 /1)	(13/ 0 /0)
	PMIWO	(12/ 0 1)	(12/ 0 /1)	(12/ 0 /1)	(13/ 0 /0)
	BGWO	(13/ 0 /0)	(11/ 0 /2)	(11/ 0 /2)	(12/ 0 /1)
	ISHADE	(9/ 2 /2)	(11/1 /1)	(10/ 2 /1)	(11/ 0 /2)
	ISSA	(13/ 0 /0)	(13/ 0 /0)	(12/ 1 /0)	(12/ 0 /1)
	Overall (+/ = /-)	(146/ 8 /15)	(149/ 8 /12)	(151/7 /11)	(151/ 6 /12)

5) ANALYSIS OF STATISTICAL RESULTS

Although the advantages of PFOA have been confirmed by comparing the optimal value, the mean and the standard deviation, a significance test is still needed to verify the difference between the proposed algorithm and its competitors. In summary, there are two types of significance tests: parametric and non-parametric. Parametric tests require that the form of the overall distribution is known, but in numerical analysis it is often difficult to make simple assumptions about the shape of the overall distribution, and then the method of parametric testing is no longer applicable. Therefore, this paper uses non-parametric tests to assess the significance of the algorithm.

First, the Wilcoxon rank sum test [40] was used to verify whether there were significant differences between this algorithm and the others. The significance level of the Wilcoxon rank sum test is set at 0.05, and the following Table 7. shows the results of the Wilcoxon rank sum test for the standard test functions F1-13 in 30, 50 and 100 dimensions and the standard test functions F14-23 in fixed dimensions. where "+/=/−" indicates a difference in performance, similar performance or no difference in performance between PFOA's performance and the comparison algorithm, respectively. Statistics of more than 10 algorithms, according to Table 7 The statistical results show that in the vast majority of cases, there are significant differences between the proposed PFOA and its competitors, with results of (146/ 8 /15), (149/ 8 /12), (151/ 7 /11) and (151/ 6 /12), respectively, and the differences are gradually widened as the dimensionality increases, verifying the performance of the algorithm It also verifies that the algorithm is suitable for higher dimensional environments.

TABLE 8. Friedman test statistical results.

			SAO	CSA	HBA	DOA	CHOA	RSO	PSO	BAS	FOA	PMIWO	BGWO	ISHADE	ISSA	PFOA
F1-F13	Dim=30	Friedman value	7.51	11.57	3.79	6.37	8.17	4.34	9.44	11.06	11.89	10.13	5.14	5.26	8.62	**3.21**
		Friedman rank	7	13	2	6	8	3	10	11	14	12	4	5	9	1
	Dim=50	Friedman value	8.22	11.87	3.84	7.74	7.65	4.72	10.89	11.08	12.37	12.23	5.78	5.67	9.34	**2.66**
		Friedman rank	9	13	2	8	7	3	11	12	14	13	5	4	10	1
	Dim=100	Friedman value	6.47	11.39	3.65	5.25	6.79	4.13	11.14	8.75	13.27	13.17	5.98	6.10	10.24	**2.61**
		Friedman rank	7	12	2	4	8	3	11	9	14	13	5	6	10	1
F14-F23	Fixed-Dim	Friedman value	11.82	4.18	6.91	7.94	10.94	12.79	4.92	13.00	8.67	8.45	6.39	7.54	5.81	**3.67**
		Friedman rank	12	2	6	8	11	13	3	14	10	9	5	7	4	1

The performance of the different optimizers in four different environments (Dim = 30, 50, 100 and fixed dimensionality) was then evaluated and ranked according to the Friedman test [41]. Table 8 shows the results of the Friedman test, and the results show that the proposed PFOA always obtains the first ranking in the case of the four different dimensions.

In summary, the PFOA proposed in this paper is a powerful optimizer that has the ability to compete with the latest and best algorithms.

IV. EXPERIMENTAL RESULTS FOR PRACTICAL ENGINEERING PROBLEMS

To verify its general applicability, PFOA was applied to four real engineering optimization problems to test the optimization results. The execution steps of the algorithm and the treatment of constraints are as follows:

First, an initial set of solutions is randomly generated that meet the design requirements (constraints). Where, Creating initialized populations that avoid constraint violations is a key factor in the successful operation of PFOA during experiments. 1) randomly generate an initial population within the range of values of each decision variable. 2) Using the penalty function method, a penalty term e^{2s} $=e^{-8}$ is added to the objective function. If a randomly generated individual satisfies the constraint, the value of the penalty function is zero and the individual is added to the initial population; if a randomly generated individual does not satisfy the constraint, the value of the penalty function becomes infinite, penalizing solutions that violate the constraint and achieving the role of screening feasible initial solutions.

Then, at each iteration of the algorithm, the fitness of the population is evaluated against the objectives and constraints, and the next generation of populations is generated based on the calculated fitness function. In other words, the algorithm will use the fitness of the current population to determine the search space for the problem.

A. THREE-BAR TRUSS DESIGN PROBLEM

This case considers a three-bar planar truss structure [42] shown in Figure 13. The volume of a statically loaded three-bar truss is to be minimized subject to stress (σ) constraints on each of the truss members. The objective is to evaluate the optimal cross-sectional areas, A_1 (equivalent to the independent variable X_1 in the formula) and A_2 (same as X_2). The mathematical formulation is given below:

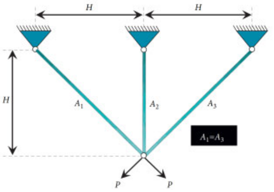

FIGURE 13. A schematic model of three-bar truss.

$$\text{minimize: } F(X) = \left(2\sqrt{2}X_1 + X_2\right) \times l \quad l = 100\text{ cm}$$

$$\text{subject to: } G_1(X) = \frac{\sqrt{2}X_1 + X_2}{\sqrt{2}X_1^2 + 2X_1X_2}P - \sigma \leq 0$$

$$P = 2\text{kN/cm}^3$$

$$G_2(X) = \frac{X_2}{\sqrt{2}X_1^2 + 2X_1X_2}P - \sigma \leq 0$$

$$\sigma = 2\text{kN/cm}^3$$

$$G_3(X) = \frac{1}{\sqrt{2}X_2 + X_1}P - \sigma \leq 0$$

$$\text{variable range: } 0 \leq X_1X_2 \leq 1$$

The optimum values for solving the three-bar planar truss structure optimization problem using different methods are shown in Table 9. and the statistical results for several optimization methods are given in Table 10. In comparison, the optimal value of PFOA is comparable or more effective than the other methods, and the number of function evaluations (NFEs) of this algorithm is 1.8E+04, which is lower than or equal to several of the remaining optimizers. For example, PSO, WSA, ICA, SSA and PFOA all find optimal values that satisfy the constraints to an accuracy of 8 decimal places, while at the same time, the PFOA algorithm finds better quality solutions without increasing the number of function evaluations (NFEs).

B. OPTIMAL DESIGN OF I-SHAPED BEAM

The second typical engineering optimization problem is the I-beam design problem [43], which aims to minimize the

TABLE 9. Best results of the three-bar truss design problem.

Algorithm	Worst	Mean	Best	STD	NFEs
GWO	263.90421778	263.89795501	263.89600631	1.61422E-03	5E+04
PSO	264.58490296	263.95741428	263.89584341	1.36897E-01	5E+04
GA	264.82080546	263.96803663	263.89588573	1.66862E-01	5E+04
WSA	263.89743217	263.89606687	263.89584342	3.11960E-04	5E+04
ICA	263.91413326	263.89932689	263.89584519	4.11693E-03	5E+04
CS	NA	264.06693742	263.97156372	9.00000E-05	1.8E+04
SSA	263.92764325	263.91174334	263.89584343	1.58999E-02	1.8E+04
PFOA	263.89584363	263.89584263	**263.89584162**	2.00641E-06	1.8E+04

TABLE 10. Comparative results for the three-bar truss design.

Algorithm	Variables		Constraints			
	X_1	X_2	G_1(X)	G_2(X)	G_3(X)	F(X)
GWO	0.788 64	0.4083	3.3400E -08	-1.464014397	-0.535985569	263.89600 63
PSO	0.788 66	0.40826	4.8650E -07	-1.464082376	-0.535917137	263.89584 34
GA	0.788 91	0.40756	9.6430E -07	-1.464873605	-0.535125421	263.89588 57
WSA	0.788 68	0.40822	- 7.2400E -07	-1.464126180	-0.535874543	263.89584 34
ICA	0.788 62	0.40838	8.4180E -07	-1.463941244	-0.536057913	263.89584 52
CS	0.788 67	0.40902	- 2.9000E -04	-0.268531643	-0.731764252	263.97165 31
SSA	0.788 66	0.40827	3.0000E -10	-1.464070360	-0.535929633	263.89584 34
PFOA	0.788 68	0.40820	1.4331E -08	-1.464146426	-0.535853559	**263.89584 16**

vertical deflection of the beam shown in Figure 14. It simultaneously satisfies the cross-sectional area and stress constraints under given loads. The width of flange b (same as X_1), the height of section h $(= X_2)$, the thickness of the web t_w $(= X_3)$, and the thickness of the flange t_f $(= X_4)$ are variables of this problem. The maximum vertical deflection of the beam is f(x) = PL^3/48EI when the length of the beam (L) and modulus of elasticity (E) are 5200 cm and 523.104 kN/cm^2, respectively. The objective function and constraints of this problem are formulated as follows:

minimize:

$$F\ (X) = \frac{5000}{X_3\ (X_2 - 2X_4)^3/12 + \left(X_1 X_4^3/6\right) + 2bX_4\ \left(X_2 - X_4/2\right)^2}$$

$$\text{subject to: } G_1\ (X) = 2X_1X_3 + X_3\ (X_2 - 2X_4) \leq 300$$

$$G_2\ (X) = \frac{18X_2 \times 10^4}{X_3\ (X_2 - 2X_4)^3 + 2X_1X_3\ \left(4X_4^2 + 3X_2\ (X_2 - 2X_4)\right)} + \frac{15X_1 \times 10^3}{(X_2 - 2X_4)\, X_3^2 + 2X_3X_1^3} \leq 56$$

$$\text{variable range: } 10 \leq X_1 \leq 50 \quad 10 \leq X_2 \leq 800$$

$$10 \leq X_2 \leq 800 \quad 9 \leq X_4 \leq 5$$

As can be observed from the best results in Table 11 many optimizers have solved this nonlinearly constrained optimization problem. In addition, Table 12 provides a comparison of the performance of the PFOA algorithm with other optimizers.In this case study, the number of function evaluations (NFEs) of the PFOA algorithm is 2.4E+04 and the standard deviation STD is 2.045E-09, two evaluation parameters that are much lower than other optimizers and show better performance.

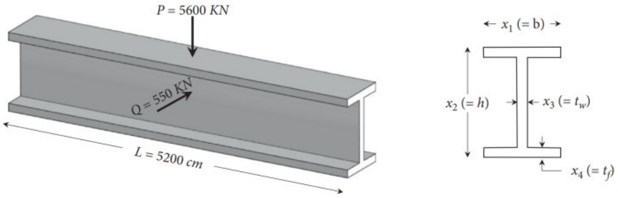

FIGURE 14. A 3D view of beam design problem.

TABLE 11. Best results for the optimal design of I-shaped beam.

Algorit hm	Variables				Constraints		
	X_1	X_2	X_3	X_4	G_1(X)	G_2(X)	F(X)
GWO	80	50	0.9	2.3217	-0.0090	-1.570071	0.0131
CS	80	50	0.9	2.3216	-0.0120	-1.570020	0.01307
SOS	80	50	0.9	2.3217	-0.0002	-1.570224	0.01307
SNS	80	50	0.9	2.3217	0	-1.570228	0.0130741
EMG O- FCR	80	50	0.9	2.3200	-0.1760	-1.567179	0.0131
AEFA- C	79.96	49.99	0.9	2.3164	-0.5603	-1.559518	0.0131
IARS M	79.99	48.42	0.9	2.4	0.08699	-1.524540	0.0131
PFOA	80	49.99	0.9	2.3218	0	-1.570219	**0.0130741 23**

TABLE 12. The other methods for the I-shaped beam problem.

Algorithm	Worst	Mean	Best	STD	NFEs
SOS	NA	1.30884E-02	1.30741E-02	4.000E- 05	5E+04
CS	1.35364E-02	1.30884E-02	1.30747E-02	1.345E- 04	5E+04
AOS	1.38140E-02	1.31788E-02	1.30741E-02	1.555E- 04	5E+04
SNS	1.30764E-02	1.30743E-02	1.30741E-02	4.313E- 07	5E+04
PFOA	1.3074123E- 02	1.3074121E- 02	1.3074119E- 02	2.045E- 09	**2.4E+04**

C. A REINFORCED CONCRETE BEAM DESIGN

Amir and Hasegawa [44], [45] presented a simplified optimization problem of designing a reinforced concrete beam, as shown in Figure 15. The beam is assumed to be simply supported with a span of 30 ft and subjected to a live load of 2000 lbf and a dead load of 1000 lbf, including the weight of the beam. The concrete compressive strength (σ_c) is 5 ksi, and the yield stress of the reinforcing steel (σ_y) is 50 ksi. The cost of concrete is \$0.02/in2/linear ft, and the cost of steel is \$1.0/in2/linear ft. To minimize the total cost of the structure, the area of the reinforcement As (equivalent to X_1), the width of the beam b $(= X_2)$, and the depth of the beam h $(= X_3)$ have to be determined. The structure should be proportioned to have a required strength based upon the ACI building code 318-77 as follows:

$$M_u = 0.9A_s\sigma_y\ (0.8h) \left(1.0 - 0.59\frac{A_s\sigma_y}{0.8bh\sigma_c}\right) \geq 1.4M_d + 1.7M_l$$

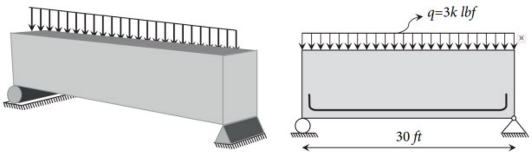

FIGURE 15. A schematic view of reinforced concrete beam.

where M_u, M_d, and M_l are the flexural strength, dead load, and live load moments of the beam, respectively. In this case, $M_d = 1350$ in kip and $M_l = 2700$ in kip. The depth to width ratio of the beam is restricted to be less than or equal to 4. The optimization problem can be expressed as:

$$\begin{aligned}
&\text{minimize: } F(X) = 2.9X_1 + 0.6X_2X_3 \\
&\text{subject to: } G_1(X) = \frac{X_2}{X_3} - 4 \leq 0 \\
&\qquad G_2(X) = 180 + 7.375\frac{X_1^2}{X_3} - X_1X_2 \leq 0 \\
&\text{variable range:} \\
&\quad X_1 \in \{6, 6.16, 6.32, 6.6, 7, 7.11, 7.2, 7.8, 7.9, 8, 8.4\} \\
&\quad X_2 \in \{28, 29, 30, \ldots, 40\} \quad 5 \leq X_3 \leq 10
\end{aligned}$$

It is clear from the constraints that X_1 and X_2 are discrete, while X_3 is continuous and is a more complex engineering optimization problem, but the PFOA algorithm achieves the optimal solution while ensuring the lowest evaluated value of the function. Table 13 gives the results of the PFOA, AOS and FA methods for this problem. PFOA, AOS, FA and SNS all find the best solution to the problem with different combinations of variables, provided that the constraints are satisfied. Table 14 compares and analyses the statistical results of PFOA, CS, FA, SNS, and AOS, and it is clear that PFOA shows its strengths in the limited number of functions evaluated.

TABLE 13. Best results of a reinforced concrete beam design.

Algorithm	Variables			Constraints		
	X_1	X_2	X_3	G_1(X)	G_2(X)	F(X)
AOS	6.32	34	8.5	-2.24094E-02	-1.00E-07	359.2080
FA	6.32	34	8.5	-2.241	0	359.2080
GA	7.20	32	8.0451	-2.8779	-0.0224	366.1459
SNS	6.32	34	8.5	2.240941E-02	5.2766E-12	359.2080
GHN-EP	6.32	34	8.6371	-0.7745	-0.0635	362.00648
PFOA	6.32	34	8.5	2.240941E-02	-4.4506E-12	359.2080

TABLE 14. Methods for a reinforced concrete beam design.

Algorithm	Worst	Mean	Best	STD	NFEs
CS	NA	NA	359.2080	NA	3E+04
FA	669.15	460.706	359.2080	80.739	3E+04
SNS	362.634	359.322	359.2080	0.6149	3E+04
AOS	362.254	359.331	359.2080	0.5961	1E+05
PFOA	362.436	359.328	359.2080	0.6051	2.4E+04

D. TUBULAR COLUMN DESIGN

This problem is an example of designing a uniform column [46] of the tubular section to carry a compressive load at minimum cost. This problem has two design variables, the mean diameter of the column d (equivalent to X_1) and the thickness of tube t (= X_2), which are shown in Figure 16. This column is made of a material with a yield stress of σ_y = 1000 kgf /cm^2 and a modulus of elasticity of $E = 0.8 \times 6 \times 10^6$ kgf /cm^2. The optimization model of this problem is given as follows:

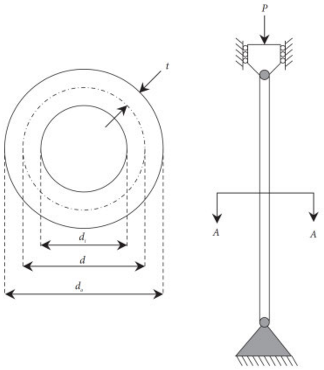

FIGURE 16. The 3D model of tubular column.

$$\begin{aligned}
&\text{minimize: } F(X) = 9.8X_1X_2 + 2X_1 \\
&\text{subject to: } G_1(X) = \frac{P}{\pi X_1 X_2 \sigma_y} - 1 \leq 0 \\
&\qquad G_2(X) = \frac{8PL^2}{\pi^3 E X_1 X_2 \left(X_1^2 + X_2^2\right)} - 1 \leq 0 \\
&\qquad G_3(X) = \frac{2.0}{X_1} - 1 \leq 0 \\
&\qquad G_4(X) = \frac{X_1}{14} - 1 \leq 0 \\
&\qquad G_5(X) = \frac{0.2}{X_2} - 1 \leq 0 \\
&\qquad G_6(X) = \frac{X_2}{8} - 1 \leq 0 \\
&\text{variable range: } 2 \leq X_1 \leq 14 \quad 0.2 \leq X_2 \leq 0.8
\end{aligned}$$

According to the constraints G_1(X) and G_2(X), the included stress in the column should be less than the buckling and yield stresses, respectively. Also, other constraints (G_3(X), G_4(X), G_5(X), and G_6(X)) clamp the variables of the problem to the ranges of the variables. Many optimizers have attempted to solve this optimization problem, comparing several existing methods with good results to PFOA. The present algorithm not only reduces the engineering cost but also effectively keeps the number of function evaluations (NFEs) below 3E+04, which is lower than other optimization algorithms, and obtains an optimum value of 26.48636152 under the constraints, as shown in Table 15. Table 16 shows the statistical results of several optimization algorithms. From these results, the PFOA algorithm achieves better results than the other algorithms, which fully demonstrates the performance of the PFOA algorithm.

TABLE 15. Best results of the tubular column design example.

	Algorithm					
	CS	ISA	FA	AOS	SNS	PFOA
X_1	5.45139	5.4511	5.45124	5.4511	5.4511562	5.45218073
X_2	0.29196	0.2919	0.29196	0.29196	0.2919654	0.29162643
$G_1(X)$	-0.0241	-2.5E-10	-0.0242	-2.49E-10	-2.6E-10	-2.049E-09
$G_2(X)$	-0.1095	-1.8E-10	-0.1093	1.8E-10	-1.8E-10	4.4415E-08
$G_3(X)$	-0.633	-0.6331	-0.633	-0.6331	-0.6331	-0.6331
$G_4(X)$	-0.610	-0.6106	-0.6109	-0.6106	-0.6106	-0.6105585
$G_5(X)$	-0.315	-0.3149	-0.3151	-0.3149	-0.3149	-0.3184
$G_6(X)$	-0.635	-0.635	-0.635	-0.635	-0.635	-0.6347430
$F(X)$	26.5321	26.531	26.52	26.531378	26.499496	26.48636152

TABLE 16. The other methods for the tubular column design.

Algorithm	Worst	Mean	Best	STD	NFEs
CS	26.53972	26.53504	26.53217	1.93E-03	3E+04
ISA	26.532	26.531	26.531	1.70E-04	3E+04
FA	NA	28.74	26.52	2.08	3E+04
SNS	26.53221	26.51585	26.49949	2.22E-06	3E+04
AOS	26.60831	26.531614	26.53138	1.03E-03	1E+05
PFOA	26.48636148	26.48636150	26.48636152	2.00E-08	2.4E+04

V. ANALYSIS AND DISCUSSION OF PFOA

The effectiveness of the PFOA algorithm can be demonstrated by the extensive experiments in the previous sections. The main tests include tests on the structure of the algorithm itself, 23 benchmark function suites in 30 dimensions 50 dimensions 100 dimensions and fixed dimensions, in addition to four tests on engineering optimization problems in non-convex scenarios combined with practical ones. PFOA and other excellent optimization algorithms together have solved about 50 optimization problems. Among them, The improved classical algorithms used for comparison are: Fruit Fly Optimization Algorithm (FOA), Particle Swarm Optimization (PSO), Beetle Antennae Search (BAS), Multi-population Invasive Weed Optimization (PMIWO), Beetle antenna strategy based grey wolf optimization (BGWO), SHADE with Linear Population Reduction (L-SHADE), Sparrow Search Algorithm Based on Lévy's Flight Perturbation Strategy(ISSA). The latest optimization algorithms for comparison are Dingo Optimization Algorithm (DOA), Chameleon Swarm Algorithm (CSA), Smell Agent Optimization (SAO), Honey Badger Algorithm (HBA), Chimp Optimization Algorithm (CHOA), Rat Swarm Optimization (RSO). This study employs a rich analytical approach, not only looking at the results in terms of optimal fitness values, means and standard deviations or convergence plots for the results of 30 multidimensional (30, 50, 100) runs, but also providing in-depth data analysis of the PFOA and comparison algorithms in terms of both box-line plots and significance.

The multi-dimensional statistics of the Wilcoxon rank sum test show significant differences between the statistical results of PFOA and the results of the above ten or so comparison algorithms. Although the latest algorithms all perform very well and are very challenging, with solutions such as RSO, WOA, HBA and DOA being relatively closer to PFOA, the performance advantages of this algorithm are further confirmed by the multi-dimensional ranking statistics of the Friedman test that follows. The data in the table shows that in all four test environments (30, 50, 100 and fixed dimensions), the first place was achieved and the Friedman test ranking value became smaller as the dimensionality of the test increased, indirectly verifying that the algorithm is suitable for higher dimensions. In terms of performance, PFOA has superior search capabilities and can efficiently converge to the global optimum position, yielding better results in less time. The algorithm effectively avoids immature convergence and stagnation problems through a non-linear parameter control strategy, a piranha population survival strategy and a reverse escape search strategy, maintaining high population diversity even at the end of the search, while exploration and exploitation levels reach a stable equilibrium. In addition, PFOA demonstrates the flexibility and universal applicability of the algorithm by solving real-world engineering design optimization problems for a much wider range of optimization problems.

VI. CONCLUSION AND OUTLOOK FOR FUTURE DEVELOPMENTS

This study proposed a novel meta-heuristic algorithm by simulating the foraging behavior of Amazonian piranhas: the Piranha Foraging Optimization Algorithm (PFOA). The objective of PFOA is to avoid falling into sub-optimal areas by efficiently traversing the search area and to balance exploration and exploitation capabilities by controlling the time-varying randomization process through the dynamics of non-linear parameters. The efficiency of the proposed PFOA was evaluated using 23 benchmark test functions as well as four engineering design problems, and the effectiveness of the search method was examined experimentally in multiple dimensions (30, 50, 100 and fixed dimensions) in terms of speed, stability and accuracy. The experimental results and convergence curves showed that PFOA is an effective algorithm for solving complex problems with high-dimension search spaces, and also confirmed the advantages of the method in terms of convergence speed, the ability to jump out of local optima and exploration and development balance. Future directions for research on PFOA include, for example, continued optimization problems for selected test functions, high-dimensional optimization problems, and optimization problems in various engineering domains.

REFERENCES

[1] D. S. Khafaga, A. A. Alhussan, E.-S.-M. El-Kenawy, A. Ibrahim, M. M. Eid, and A. A. Abdelhamid, "Solving optimization problems of metamaterial and double T-shape antennas using advanced meta-heuristics algorithms," *IEEE Access*, vol. 10, pp. 74449–74471, 2022.

[2] S. Lin, A. Liu, J. Wang, and X. Kong, "An intelligence-based hybrid PSO-SA for mobile robot path planning in warehouse," *J. Comput. Sci.*, vol. 67, Mar. 2023, Art. no. 101938.

[3] A. Banerjee, S. K. De, and K. Majumder, "Construction of effective wireless sensor network for smart communication using modified ant colony optimization technique," in *Advanced Computing and Intelligent Technologies*, vol. 218. Singapore: Springer, Jul. 2022, pp. 269–278.

[4] A. Qi, D. Zhao, F. Yu, A. A. Heidari, Z. Wu, Z. Cai, F. Alenezi, R. F. Mansour, H. Chen, and M. Chen, "Directional mutation and crossover boosted ant colony optimization with application to COVID-19 X-ray image segmentation," *Comput. Biol. Med.*, vol. 148, Sep. 2022, Art. no. 105810.

[5] O. N. Oyelade, A. E.-S. Ezugwu, T. I. A. Mohamed, and L. Abualigah, "Ebola optimization search algorithm: A new nature-inspired metaheuristic optimization algorithm," *IEEE Access*, vol. 10, pp. 16150–16177, 2022.

[6] E. Bonabeau, M. Dorigo, and G. Theraulaz, "Inspiration for optimization from social insect behavior," *Nature*, vol. 406, no. 6791, pp. 39–42, Jul. 2000.

[7] R. Eberhart and J. Kennedy, "A new optimizer using particle swarm theory," in *Proc. Micro Mach. Hum. Sci.*, Apr. 1995, pp. 39–43.

[8] F. A. Hashim, E. H. Houssein, K. Hussain, M. S. Mabrouk, and W. Al-Atabany, "Honey badger algorithm: New metaheuristic algorithm for solving optimization problems," *Math. Comput. Simul.*, vol. 192, pp. 84–110, Feb. 2022.

[9] M. S. Braik, "Chameleon Swarm algorithm: A bio-inspired optimizer for solving engineering design problems," *Expert Syst. Appl.*, vol. 174, Jul. 2021, Art. no. 114685.

[10] S. Forrest, "Genetic algorithms," *ACM Comput. Surv.*, vol. 28, no. 1, pp. 77–80, 1996.

[11] J. Vesterstrom and R. Thomsen, "A comparative study of differential evolution, particle swarm optimization, and evolutionary algorithms on numerical benchmark problems," in *Proc. Congr. Evol. Comput.*, vol. 2, Jun. 2004, pp. 1980–1987.

[12] L. Bertolini, "Complex systems, evolutionary planning?" in *Planner's Encounter with Complexity*. Evanston, IL, USA: Routledge, 2016, pp. 81–98.

[13] H.-G. Beyer and H.-P. Schwefel, "Evolution strategies-a comprehensive introduction," *Natural Comput.*, vol. 1, no. 1, pp. 3–52, 2002.

[14] P. J. Van Laarhoven, E. H. Aarts, and P. J. van Laarhoven, *Simulated Annealing*. Amsterdam, The Netherlands: Springer, 1987, pp. 7–15.

[15] A. Kaveh and A. Dadras, "A novel meta-heuristic optimization algorithm: Thermal exchange optimization," *Adv. Eng. Softw.*, vol. 110, pp. 69–84, Aug. 2017.

[16] H. Peraza-Vázquez, A. F. Peña-Delgado, G. Echavarría-Castillo, A. B. Morales-Cepeda, J. Velasco-Álvarez, and F. Ruiz-Perez, "A bio-inspired method for engineering design optimization inspired by dingoes hunting strategies," *Math. Problems Eng.*, vol. 2021, pp. 1–19, Sep. 2021.

[17] B. Deng, "An improved honey badger algorithm by genetic algorithm and levy flight distribution for solving airline crew rostering problem," *IEEE Access*, vol. 10, pp. 108075–108088, 2022.

[18] A. T. Salawudeen, M. B. Mu'azu, Y. A. Sha'aban, and A. E. Adedokun, "A novel smell agent optimization (SAO): An extensive CEC study and engineering application," *Knowl.-Based Syst.*, vol. 232, Nov. 2021, Art. no. 107486.

[19] M. Khishe and M. R. Mosavi, "Chimp optimization algorithm," *Expert Syst. Appl.*, vol. 149, Jul. 2020, Art. no. 113338.

[20] G. Dhiman, M. Garg, A. Nagar, V. Kumar, and M. Dehghani, "A novel algorithm for global optimization: Rat swarm optimizer," *J. Ambient Intell. Humanized Comput.*, vol. 12, no. 8, pp. 8457–8482, Aug. 2021.

[21] H. Chen, A. A. Heidari, H. Chen, M. Wang, Z. Pan, and A. H. Gandomi, "Multi-population differential evolution-assisted Harris hawks optimization: Framework and case studies," *Future Gener. Comput. Syst.*, vol. 111, pp. 175–198, Oct. 2020.

[22] R. J. Kuo, Y. H. Lee, F. E. Zulvia, and F. C. Tien, "Solving bi-level linear programming problem through hybrid of immune genetic algorithm and particle swarm optimization algorithm," *Appl. Math. Comput.*, vol. 266, pp. 1013–1026, Sep. 2015.

[23] Q. Fan, H. Huang, Y. Li, Z. Han, Y. Hu, and D. Huang, "Beetle antenna strategy based grey wolf optimization," *Expert Syst. Appl.*, vol. 165, Mar. 2021, Art. no. 113882.

[24] E. V. Altay and B. Alatas, "Bird swarm algorithms with chaotic mapping," *Artif. Intell. Rev.*, vol. 53, no. 2, pp. 1373–1414, Feb. 2020.

[25] D. Zhao, A. Qi, F. Yu, A. A. Heidari, H. Chen, and Y. Li, "Multi-strategy ant colony optimization for multi-level image segmentation: Case study of melanoma," *Biomed. Signal Process. Control*, vol. 83, May 2023, Art. no. 104647.

[26] A. K. Singh and A. Kumar, "An improved dynamic weighted particle swarm optimization (IDW-PSO) for continuous optimization problem," *Int. J. Syst. Assurance Eng. Manage.*, vol. 14, pp. 1–15, Jan. 2023.

[27] M. Parvin, H. Yousefi, and Y. Noorollahi, "Techno-economic optimization of a renewable micro grid using multi-objective particle swarm optimization algorithm," *Energy Convers. Manage.*, vol. 277, Feb. 2023, Art. no. 116639.

[28] S. P. Adam, S. A. N. Alexandropoulos, and P. M. Pardalos, "No free lunch theorem: A review," *Approximation Optim.*, vol. 145, pp. 57–82, May 2019.

[29] I. Sazima and F. A. Machado, "Underwater observations of piranhas in western Brazil," in *Alternative Life-History Styles of Fishes*, vol. 10. Dordrecht, The Netherlands: Springer, 1990, pp. 17–31.

[30] X. Raick, A. Huby, G. Kurchevski, A. L. Godinho, and É. Parmentier, "Use of bioacoustics in species identification: Piranhas from genus *Pygocentrus* (Teleostei: Serrasalmidae) as a case study," *PLoS ONE*, vol. 15, no. 10, Oct. 2020, Art. no. e0241316.

[31] R. P. Shellis and B. K. B. Berkovitz, "Observations on the dental anatomy of piranhas (Characidae) with special reference to tooth structure," *J. Zool.*, vol. 180, no. 1, pp. 69–84, Sep. 1976.

[32] M. Banse, B. P. Chagnaud, A. Huby, E. Parmentier, and L. Kéver, "Sound production in piranhas is associated with modifications of the spinal locomotor pattern," *J. Experim. Biol.*, vol. 224, no. 9, May 2021, Art. no. jeb242336.

[33] S. Dhargupta, M. Ghosh, S. Mirjalili, and R. Sarkar, "Selective opposition based grey wolf optimization," *Expert Syst. Appl.*, vol. 151, Aug. 2020, Art. no. 113389.

[34] X. Jiang and S. Li, "BAS: Beetle antennae search algorithm for optimization problems," 2017, *arXiv:1710.10724*.

[35] H. Chen, Y.-Q. Zhou, and G.-W. Zhao, "Multi-population invasive weed optimization algorithm based on chaotic sequence," *J. Comput. Appl.*, vol. 32, no. 6, pp. 1958–1961, Aug. 2013.

[36] R. Tanabe and A. S. Fukunaga, "Improving the search performance of SHADE using linear population size reduction," in *Proc. IEEE Congr. Evol. Comput. (CEC)*, Jul. 2014, pp. 1658–1665.

[37] W. Mao and X. Zhao, "A sparrow search algorithm based on Lévy's flight perturbation strategy," *J. Appl. Sci.*, vol. 40, no. 1, pp. 1–15, 2022.

[38] L. G. Tallini, D. Pelusi, R. Mascella, L. Pezza, S. Elmougy, and B. Bose, "Efficient non-recursive design of second-order spectral-null codes," *IEEE Trans. Inf. Theory*, vol. 62, no. 6, pp. 3084–3102, Jun. 2016.

[39] M. Spitzer, J. Wildenhain, J. Rappsilber, and M. Tyers, "BoxPlotR: A web tool for generation of box plots," *Nature Methods*, vol. 11, no. 2, pp. 121–122, Jan. 2014.

[40] P. D. Bridge and S. S. Sawilowsky, "Increasing physicians' awareness of the impact of statistics on research outcomes: Comparative power of the t-test and Wilcoxon rank-sum test in small samples applied research," *J. Clin. Epidemiol.*, vol. 52, no. 3, pp. 229–235, Mar. 1999.

[41] T. H. Li, M. X. Dan, and Z. D. Yu, "Enhanced sparrow search algorithm based on multiple improved strategies," *J. Comput. Appl.*, Nov. 2022, doi: 10.11772/j.issn.1001-9081.2022081270.

[42] H. Fauzi and U. Batool, "A three-bar truss design using single-solution simulated Kalman filter optimizer," *MEKATRONIKA*, vol. 1, no. 2, pp. 98–102, Jul. 2019.

[43] T.-T. Nguyen and J. Lee, "Optimal design of thin-walled functionally graded beams for buckling problems," *Compos. Struct.*, vol. 179, pp. 459–467, Nov. 2017.

[44] A. Kaveh and K. B. Hamedani, "Improved arithmetic optimization algorithm and its application to discrete structural optimization," *Structures*, vol. 35, pp. 748–764, Jan. 2022.

[45] J. Waheed, R. Azam, M. R. Riaz, M. Shakeel, A. Mohamed, and E. Ali, "Metaheuristic-based practical tool for optimal design of reinforced concrete isolated footings: Development and application for parametric investigation," *Buildings*, vol. 12, no. 4, p. 471, Apr. 2022.

[46] Y. Kurobane, K. Ogawa, and K. Ochi, "Recent research developments in the design of tubular structures," *J. Constructional Steel Res.*, vol. 13, nos. 2–3, pp. 169–188, Jan. 1989.

SHUAI CAO was born in Baotou, Inner Mongolia, in 1998. He received the degree in electronic information engineering. He is currently pursuing the master's degree with the School of Information Engineering and Automation, Kunming University of Science and Technology.

Since September 2021, he has been a Research Assistant with the Computer Key Laboratory, Kunming University of Science and Technology. Since July 2022, he has also been an Engineer with the Robotics Laboratory, South China Intelligent Robot Innovation Institute. His research interests include intelligent optimization algorithm, bionic algorithm, and engineering optimization.

QIAN QIAN was born in October 1981. From January to March 2017, he was with the Kochi University of Technology, Japan, as a Guest Associate Professor, for short-term exchange, and went to Tohoku University, Chiba University, and the Kanazawa University of Technology, for research publication and exchange. He is currently a Professor with the Faculty of Information Engineering and Automation, Kunming University of Science and Technology. He has presided over two National Natural Science Foundation projects, one surface project of the Science and Technology Department of Yunnan Province, one key project of the Education Department of Yunnan Province, and one international cooperation project with the Kochi University of Science and Technology. As the first author, he has published nearly ten academic articles retrieved by SSCI in domestic and foreign academic journals with high-impact factors. His research interests include visual cognition and cognitive computing models, and computational intelligence.

YONGJUN CAO is a professor-level Senior Engineer and a Graduate Supervisor. He is currently the Dean of the South China Robotics Innovation Research Institute and the Vice Dean of the Institute of Intelligent Manufacturing, Guangdong Academy of Sciences. In recent years, he had undertaken nearly 20 national, provincial, and municipal science and technology projects. In the field of intelligent production lines, he had applied more than 60 patents, granted 30 patents, participated in one national standard of industrial robot control, and published more than 20 articles. His research interests include intelligent control and vision, precision equipment and embedded robots, flexible intelligence, and complex systems.

He is a member of the Guangdong Automation System and Integration Standard Committee and the Director and the Deputy Secretary General of the Guangdong Mechanical Engineering Society and the Guangdong Automation Association.

WENWEI LI was born in Jilin, China, in 1981. He received the Ph.D. degree in mechanical engineering from Southeast University, in 2012. After graduation, he was with the Hefei Institute of Physical Sciences, Chinese Academy of Sciences (CAS). Since 2018, he has been with the South China Robotic Innovation Research Institute (SCRI), where he is currently a Senior Engineer. He has hosted some key projects and invited as a reviewer for several international conferences. He had published 22 papers, granted 12 patents, and registered two software copyrights. His research interests include intelligent robot, CAD/CAE based on simulation and optimization, machinery dynamics, and manufacturing information systems.

WEIXI HUANG was born in Shanwei, Guangdong, China, in 1983. He received the M.S. degree in optical engineering from Jinan University, Guangzhou, in 2010.

From 2010 to 2011, he was a Research and Development Engineer with Oplink, Zhuhai. Since 2020, he has been the Head of Science and Technology Business with the South China Robotics Innovation Research Institute, Foshan. He is responsible for the overall scientific and technological development of the institute, especially the application of advanced computer technology in industrial manufacturing, such as the research of machine vision technology and visual algorithm model.

JIANAN LIANG was born in Xi'an, Shaanxi, China. He received the master's degree. He is currently an Engineer with the Institute of Intelligent Manufacturing, Guangdong Academy of Sciences. He has published nine academic articles related to robot and machine vision, including one SCI paper and nearly 30 invention patents. His research interests include machine vision, intelligent control, mechatronics, robot application, and other technologies.